

Manuscript Number:

Title: Magnetocaloric effect and magnetic properties crystals of  $RA_2$  (R: Dy, Ho, Er) calculated by ATOMIC MATTERS MFA Computation System.

Article Type: Research Paper

Keywords:  $RA_2$ , Laves Phase, CEF, MFA, MCE, Atomic Matters.

Corresponding Author: Dr. Rafał Michalski,

Corresponding Author's Institution: INDUFORCE Rafał Michalski

First Author: Rafał Michalski

Order of Authors: Rafał Michalski; Jakub Zygadło; Tomasz Lanczewski

Abstract: We present the results of calculations of magnetic properties of 3 compounds from Laves phase  $C15$  family:  $DyAl_2$ ,  $HoAl_2$  and  $ErAl_2$  performed with our new computation system called ATOMIC MATTERS MFA. The calculation methodology was based on localized electron approach applied to describe the thermal evolution electronic structure of rare-earth  $R^{3+}$  ions over a wide temperature range and estimate Magnetocaloric Effect (MCE). Thermomagnetic properties were calculated based on the fine electronic structure of the  $4f^9$ ,  $4f^{10}$  and  $4f^{11}$  configuration of the  $Dy^{3+}$ ,  $Ho^{3+}$ ,  $Er^{3+}$  ions respectively. Our calculations yielded: magnetic moment value and direction; single-crystalline magnetization curves in zero field and in external magnetic field applied in various directions  $m(T, B_{ext})$ ; the  $4f$ -electronic components of specific heat  $c_{4f}(T, B_{ext})$ ; and temperature dependence of the magnetic entropy and isothermal entropy change with external magnetic field  $-T\Delta S(T, B_{ext})$ . The cubic CEF parameters values used for  $DyAl_2$  calculations was taken from earlier research of A. L. Lima, A. O. Tsokol and recalculated for universal cubic parameters ( $A_{mn}$ ) for the  $RA_2$  series. Our studies reveal the importance of multipolar charge interactions when describing thermomagnetic properties of real  $4f$  electronic systems and the effectiveness of an applied self-consistent molecular field in calculations for magnetic phase transition simulation.

# COVER LETTER

## Title:

Magnetocaloric effect and magnetic properties crystals of  $RAI_2$  (R: Dy, Ho, Er) calculated by ATOMIC MATTERS MFA Computation System

## Authors:

1. Rafał Michalski, Atomic Systems, M. Pszona 41/29, Cracow, Poland
2. Jakub Zygadło, Faculty of Mathematics and Computer Science, Jagiellonian University, Cracow, Poland
3. Tomasz Lanczewski, Atomic Systems, M. Pszona 41/29, Cracow, Poland

**Short statement of the problem:** Results of our recent calculations of properties of  $RAI_2$  crystals are presented. Our calculations yielded: vector of magnetic moment; single-crystalline magnetization curves in external magnetic field applied in various directions  $\mathbf{m}(T, \mathbf{B}_{\text{ext}})$ ;  $4f$ - specific heat  $c_{4f}(T, \mathbf{B}_{\text{ext}})$ ; and temperature dependence of the magnetic entropy and entropy change with external magnetic field  $-\Delta S(T, \mathbf{B}_{\text{ext}})$ .

**Brief description of the approach:** We applied localized electron approach to describe the thermal evolution of Fine Electronic Structure of  $Dy^{3+}$ ,  $Ho^{3+}$  and  $Er^{3+}$  ions over a wide temperature range and estimate Magnetocaloric Effect (MCE) by with our new computation system ATOMIC MATTERS MFA. Thermomagnetic properties of  $DyAl_2$ ,  $HoAl_2$  and  $ErAl_2$  were calculated based on the fine electronic structure of the  $4f^8$ ,  $4f^7$  and  $4f^6$  electronic configuration of the  $Dy^{3+}$  and  $Ho^{3+}$  and  $Er^{3+}$  ions, respectively. The cubic universal CEF parameters values used for all CEF calculations was taken from literature and recalculated for universal cubic parameters set for the  $RAI_2$  series:  $A_4=+7.164Ka_0$  and  $A_6=-1.038Ka_0$ .

**List of novel contributions:** Creating of consistent description of properties of compounds  $DyAl_2$ ,  $HoAl_2$  and  $ErAl_2$ . Establishing molecular field factors for those compounds. Postulating spin and orbital moment compensation in  $SmAl_2$  compounds as reason of its unusual behavior.

**List of other papers with content overlap:** none

## A reference to the closest prior article:

J.J.M. Franse, R.J. Radwanski, Magnetic properties of binary rare-earth... in *Handbook of Magnetic Materials* Vol. 7, edited K.H.J. Bushow (1993) 307-500.

## Experts in the field:

Prof. J.J.M. Franse,  
Prof. R.J. Radwanski,  
Prof. P.J. von Ranke  
Prof. V.K. Pecharsky

## \*Potential Reviewers

Suggesting 4 reviewers

Donald Galvan, Universidad Nacional Autonoma de Mexico, [donald@cryn.unam.mx](mailto:donald@cryn.unam.mx), Excellent scientist in the area of Solid State Physics.

Olivier Isnard, Neel Institute Grenoble, France, [olivier.isnard@neel.cnrs.fr](mailto:olivier.isnard@neel.cnrs.fr) Excellent scientist in the area of Solid State Physics.

Ryszard Radwanski, UP, Kraków Poland, [sfradwan@cyf-kr.edu.pl](mailto:sfradwan@cyf-kr.edu.pl), Excellent scientist in the area of Solid State Physics.

Bartłomiej Szafran, AGH, Kraków Poland, [bszafran@agh.edu.pl](mailto:bszafran@agh.edu.pl), Excellent scientist in the area of Quantum Mechanics.

# Magnetocaloric effect and magnetic properties crystals of $\text{RAl}_2$ (R: Dy, Ho, Er) calculated by ATOMIC MATTERS MFA Computation System

R Michalski<sup>1</sup> and J Zygadlo<sup>2</sup>

<sup>1</sup>Atomic Systems, M. Pszozna 41/29, 31-462 Cracow, Poland

<sup>2</sup>Faculty of Mathematics and Computer Science, Jagiellonian University, Łojasiewicza 6, 30-348 Cracow, Poland

E-mail: r.michalski@induforce.eu

## Abstract

We present the results of calculations of magnetic properties of 3 compounds from Laves phase C15 family:  $\text{DyAl}_2$ ,  $\text{HoAl}_2$  and  $\text{ErAl}_2$  performed with our new computation system called ATOMIC MATTERS MFA. The calculation methodology was based on localized electron approach applied to describe the thermal evolution electronic structure of rare-earth  $\text{R}^{3+}$  ions over a wide temperature range and estimate Magnetocaloric Effect (MCE). Thermomagnetic properties were calculated based on the fine electronic structure of the  $4f^9$ ,  $4f^{10}$  and  $4f^{11}$  configuration of the  $\text{Dy}^{3+}$ ,  $\text{Ho}^{3+}$ ,  $\text{Er}^{3+}$  ions respectively. Our calculations yielded: magnetic moment value and direction; single-crystalline magnetization curves in zero field and in external magnetic field applied in various directions  $\mathbf{m}(\text{T}, \mathbf{B}_{\text{ext}})$ ; the  $4f$ -electronic components of specific heat  $c_{4f}(\text{T}, \mathbf{B}_{\text{ext}})$ ; and temperature dependence of the magnetic entropy and isothermal entropy change with external magnetic field  $-\Delta S(\text{T}, \mathbf{B}_{\text{ext}})$ . The cubic CEF parameters values used for  $\text{DyAl}_2$  calculations was taken from earlier research of A. L. Lima, A. O. Tsokol and recalculated for universal cubic parameters ( $A_n^m$ ) for the  $\text{RAl}_2$  series. Our studies reveal the importance of multipolar charge interactions when describing thermomagnetic properties of real  $4f$  electronic systems and the effectiveness of an applied self-consistent molecular field in calculations for magnetic phase transition simulation.

Keywords:  $\text{RAl}_2$ , Laves Phase, CEF, MFA, MCE, Atomic Matters.

## 1. Introduction

Condensed matter science research in advanced magnetic refrigerant materials has focused on the giant magnetocaloric effect since its discovery. This has advanced the development of near room-temperature magnetic cooling technology. Understanding and controlling the microscopic quantum mechanisms responsible for storing and releasing material entropy through controlled external magnetic field change processes is one of the biggest challenges in materials science.

The  $\text{RAl}_2$  (R=rare earth element) compounds are well known intermetallic materials with interesting magnetic properties at low temperatures. The magnetic properties of this series were studied intensively in the 1970s, but a new wave of interest in this compound family has appeared due to research into materials with a large Magnetocaloric Effect (MCE) for future magnetic refrigerators. We present the results of simulations performed by our ATOMIC MATTERS computation system [1,2] of thermomagnetic properties of  $\text{DyAl}_2$ . A few calculation results for the  $\text{DyAl}_2$  compound are compared with experimental data taken from the literature [3-8]. All the lanthanides combine with aluminum to form an  $\text{RAl}_2$  compound with the same crystalline structure. This structure is the so-called cubic Laves phase C15 and the point symmetry for the rare earth ion is  $4\bar{3}m$ .

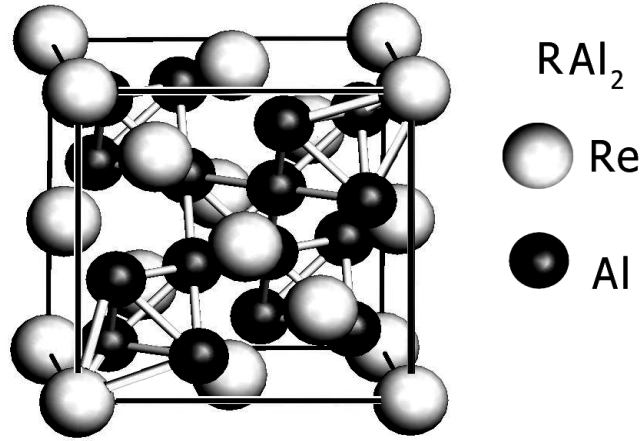


Figure 1. Cubic elementary cell of  $RAl_2$  Laves phase C15 crystals.

The structure was named after the Swiss crystallographer who performed work on the prototype compound  $MgCu_2$ . The CEF parameters describing the multipolar charge interaction of R ions in the crystal surrounding in this structure were agreed for both compounds and established by a previous study [3,4,9] for  $A_4 = +7.164K a_0$  and  $A_6 = -1.038K a_0$ .

## 2. Computation system

All  $RAl_2$  calculations were performed with ATOMIC MATTERS MFA computation system [2], an extension of the ATOMIC MATTERS application [1] that describes fine electronic structure and predicts basic magnetic and spectral properties of materials in a paramagnetic state. ATOMIC MATTERS MFA calculates magnetic, calorimetric and spectroscopic properties of atomic-like localized electron systems under the influence of Crystal Electric Field (CEF), spin-orbit coupling, and magnetic interactions, taken both as Mean Field Approximation (MFA) self-consistent, dynamic calculations and the influence of established external magnetic fields  $\mathbf{B}_{ext}$  [2]. ATOMIC MATTERS MFA calculates macroscopic properties of materials in defined temperature regions, especially around phase transition temperature, such as: magnetic moment  $\mathbf{m}(T, \mathbf{B}_{ext})$  (spin and orbital, directional components); localized electron specific heat  $c_{4f}(T, \mathbf{B}_{ext})$ ; localized electron entropy with a useful tool set for MCE; isothermal entropy change  $-\Delta S(T, \mathbf{B}_{ext})$  calculations; evolution of energy level positions; total free energy.

Both calculation systems contain advanced Graphic User Interface (GUI) with system of hierarchical tabs for calculation results management, 3D interactive visualizations of potentials and fields based on Open GL graphic engine, tools and databases for convenient and effective work. More in-date information about Atomic Matters computation systems are available on our web page [10].

## 3. Theoretical background

The theoretical approach applied at the heart of ATOMIC MATTERS MFA computation system is deeply rooted in atomic physics. Taking into consideration the individual population of states of fine electronic structure of ions/atoms at different temperatures according to L. Boltzmann statistics make it possible to define the temperature dependencies of single ionic properties. ATOMIC MATTERS MFA can simulate phase transitions of ionic/atomic systems according to dynamic calculations of the molecular field  $B_{mol}$ , simply defined as:

$$\mathbf{B}_{mol}(T) = n_{mol} \mathbf{m}(T) \quad (1)$$

This interacts with ions to induce their magnetic moments. Such self-consistent calculations can only be performed after establishing the molecular field factor  $n_{mol}$  that is closely related to the temperature of phase transitions  $T_C$ .

For rapid calculations in a thermodynamically stable temperature region, ATOMIC MATTERS offers the following CEF+Spin-Orbit+Zeeman Hamiltonian according to the chosen calculation space of ground multiplet  $|J, J_z\rangle$  or ground atomic term  $|LSL_z S_z\rangle$  respectively[1]:

$$H_J = H_{CEF} + H_{Zeeman} = \sum_n \sum_m B_n^m \hat{O}_n^m(J, J_z) + g_L \mu_B \mathbf{J} \cdot \mathbf{B}_{ext} \quad (2)$$

or

$$H_{LS} = H_{CEF} + H_{S-O} + H_{Zeeman} = \sum_n \sum_m B_n^m \hat{\mathbf{O}}_n^m(L, L_z) + \lambda \mathbf{L} \cdot \mathbf{S} + \mu_B (\mathbf{L} + g_e \mathbf{S}) \cdot \mathbf{B}_{ext} \quad (3)$$

For all Hamiltonians:  $B_n^m$  denotes CEF parameters,  $\hat{\mathbf{O}}_n^m$  are Stevens operators,  $\lambda$ -is the spin-orbit constant, and  $g_L$  and  $g_e \approx 2.002319$  are the gyromagnetic factors of a whole ion or single electron respectively. For a whole ion or electron respectively,  $\mu_B$  is the Bohr magneton and  $\mathbf{B}_{ext}$  is the external magnetic field. In all cases, calculations in the  $|\text{LSL}_z S_z\rangle$  space are more physically appropriate due to their completeness, but traditional calculations with base  $|\text{JJ}_z\rangle$  can be also performed by our computation systems for comparisons and rapid estimations [2]. For calculating properties in temperatures around the magnetic phase transition point, a self-consistent methodology for molecular field calculation called Mean Field Approximations (MFA) is applied. The idea behind this method is the estimation of direction and value of the magnetic field (molecular field) generated by ions at a defined temperature, and calculation of the influence of this magnetic field for electronic state structures of ions. In a selected calculation space, according to (1) we define a molecular field as an expected value of the total moment of the 4f electronic subshell multiplied by the molecular field, inter ionic exchange factor  $n_{mol}$ :

$$\mathbf{B}_{mol} = -n_{mol} g_L \mu_B \langle \mathbf{J} \rangle \quad (4)$$

or

$$\mathbf{B}_{mol} = -n_{mol} \mu_B \langle \mathbf{L} + g_e \mathbf{S} \rangle \quad (5)$$

Where  $g_L$  and  $g_e \approx 2.002319$  are the gyromagnetic factors. On the basis of the calculated electronic level structure  $E_i(T)$ , the directional components of magnetic moments are established for all identical ions. This means that Hamiltonian matrix diagonalization is performed for all defined temperature steps recurrently, in contrast to simple ATOMIC MATTERS calculations [1], which diagonalize matrices one time for a single run and deduce all thermodynamic properties from the stable discrete energy level structure obtained. This self-consistent procedure provides temperature-dependent energy level structure and has one only free parameter,  $n_{mol}$ , called the molecular field parameter. The value of  $n_{mol}$  is closely related to the phase transition temperature  $T_C$  of the macroscopic structure of ions. The formal expression of the full Hamiltonian used by ATOMIC MATTERS MFA computation system, according to the chosen calculation space  $|\text{JJ}_z\rangle$  or  $|\text{LSL}_z S_z\rangle$  respectively, has the form:

$$H_{J\ mol} = H_J + H_{mol} = \sum_n \sum_m B_n^m \hat{\mathbf{O}}_n^m(J, J_z) + n_{mol} g_L^2 \mu_B^2 \left( -\mathbf{J} \cdot \mathbf{J} + \frac{1}{2} \langle \mathbf{J}^2 \rangle \right) + g_L \mu_B \mathbf{J} \cdot \mathbf{B}_{ext} \quad (6)$$

or

$$H_{LS\ mol} = \sum_n \sum_m B_n^m \hat{\mathbf{O}}_n^m(L, L_z) + \lambda \mathbf{L} \cdot \mathbf{S} + n_{mol} \mu_B^2 \left( -(\mathbf{L} + g_e \mathbf{S}) \cdot (\mathbf{L} + g_e \mathbf{S}) + \frac{1}{2} \langle (\mathbf{L} + g_e \mathbf{S})^2 \rangle \right) + \mu_B (\mathbf{L} + g_e \mathbf{S}) \cdot \mathbf{B}_{ext} \quad (7)$$

The eigenvectors of the Hamiltonian are described according to the selected calculation base by the total momentum quantum numbers  $|\text{JJ}_z\rangle$  or spin and orbit quantum numbers  $|\text{LSL}_z S_z\rangle$ . Using the commutation relations of the angular momentum operators, we obtain information about expected values of the projections of magnetic momentum of all electronic states at a chosen temperature [2]:

$$m_j^a(T) = \frac{g_L \mu_B}{Z(T)} \sum_i \langle J_\alpha^i \rangle \exp\left(-\frac{E_i(T)}{k_B T}\right) \quad (8)$$

$$m_{LS}^a(T) = \frac{\mu_B}{Z(T)} \sum_i \langle L_\alpha^i + g_e S_\alpha^i \rangle \exp\left(-\frac{E_i(T)}{k_B T}\right) \quad (9)$$

Where:  $\alpha$  indexes directional components,  $i$  numbers the Hamiltonian eigenstates, while  $\Gamma_i$  represents the expected value of the total angular momentum along the  $\alpha$ -axis in the  $i$ -th state:

$$\langle J_\alpha^i \rangle = \langle \Gamma_i(T) | \mathbf{J}_\alpha | \Gamma_i(T) \rangle \quad (10)$$

$$\langle L_\alpha^i + g_e S_\alpha^i \rangle = \langle \Gamma_i(T) | \mathbf{L}_\alpha + g_e \mathbf{S}_\alpha | \Gamma_i(T) \rangle \quad (11)$$

All property calculations can be done for 3D (x,y,z) real space by using complex Hamiltonian matrix elements defined by full expressions of extended Stevens  $\hat{\mathbf{O}}_n^m$  operators[11]. Mostly for comparison with traditional calculation results, ATOMIC MATTERS also offers a 2D (x,z) calculation methodology of a simplified model of CEF interactions defined by Stevens  $\hat{\mathbf{O}}_n^m$  operators with real number matrix elements only [12].

Taking into consideration the possibility of the thermal population of states, we automatically obtain the thermal evolution of single ion properties of the whole compound [13,14].

Under the thermodynamic principle at temperature  $T=0\text{K}$  only the ground state is occupied. In this situation, the magnetic moment of the ion is exactly equal to the momentum of the ground state. If the temperature rises, the

probability of occupying higher states increases according to Boltzmann statistics. The number of ions with energy  $E_i$  within a system at temperature  $T$  is:

$$N_i(T) = N_0 \frac{\exp\left(-\frac{E_i(T)}{k_B T}\right)}{Z(T)} \quad (12)$$

where  $N_0 \approx 6.022 \cdot 10^{23} \text{ mol}^{-1}$  (Avogadro constant) and  $Z(T)$  is the sum of states. Knowing the sum of the states, we can determine the Helmholtz free energy  $F(T)$ :

$$F(T) = -k_B T \ln Z(T) \quad (13)$$

According to thermodynamic principles, the contribution of localized electrons to the total specific heat of materials can be calculated by numerical derivation of Helmholtz free energy:

$$c_{\text{mol}}(T) = -T \left( \frac{\partial^2 F(T)}{\partial T^2} \right) \quad (14)$$

This makes it possible to calculate entropy according to the well-known definition:

$$S(T) = S(0) + \int_0^T \frac{c(T)}{T} dT \quad (15)$$

The value of electronic entropy for a defined temperature is difficult to compare, but the isothermal change of the entropy of the system at a given temperature is a very important material parameter that describes its thermomagnetic properties. Isothermal Entropy change  $-\Delta S(T, B_{\text{ext}})$ , captured for different temperatures under the influence of different magnetic fields, is one the most important properties of a material that describes its usefulness as a magnetocaloric material. The value  $-\Delta S(T, B_{\text{ext}})$ , which was extracted from experimental specific heat measurements, is often presented as a basic description of the Magnetocaloric Effect (MCE) of a material [3-7]. In our approach, isothermal entropy change can be directly calculated from (15) according to the definition:

$$\Delta S(T, B_{\text{ext}}) = S(T, B_{\text{ext}}=0) - S(T, B_{\text{ext}}). \quad (16)$$

ATOMIC MATTERS MFA also provides single-ionic magnetocrystalline anisotropy calculations that include full calculations (without Brillouin function approximation) of  $K_i(T)$  magnetocrystalline constants for defined temperature ranges according to the relations [15]:

$$\begin{aligned} K_1(T) &= \frac{3}{2} B_2^0 (\langle \hat{\mathbf{O}}_2^0 \rangle - \langle \hat{\mathbf{O}}_2^2 \rangle) - 5 B_4^0 (\langle \hat{\mathbf{O}}_4^0 \rangle - 3 \langle \hat{\mathbf{O}}_4^2 \rangle) - \frac{21}{2} B_6^0 (\langle \hat{\mathbf{O}}_6^0 \rangle - 5 \langle \hat{\mathbf{O}}_6^2 \rangle), \\ K_2(T) &= \frac{35}{8} B_4^0 (\langle \hat{\mathbf{O}}_4^0 \rangle - 4 \langle \hat{\mathbf{O}}_4^2 \rangle + \langle \hat{\mathbf{O}}_4^4 \rangle) + \frac{63}{8} B_6^0 (\langle \hat{\mathbf{O}}_6^0 \rangle - 20 \langle \hat{\mathbf{O}}_6^2 \rangle + 5 \langle \hat{\mathbf{O}}_6^4 \rangle), \\ K_2^*(T) &= \frac{1}{8} (B_4^0 \langle \hat{\mathbf{O}}_4^0 \rangle + 5 B_6^0 \langle \hat{\mathbf{O}}_6^4 \rangle), \quad K_3(T) = -\frac{231}{16} B_6^0 \langle \hat{\mathbf{O}}_6^0 \rangle, \quad K_3^*(T) = -\frac{11}{16} B_6^0 \langle \hat{\mathbf{O}}_6^4 \rangle. \end{aligned} \quad (17)$$

Where:  $\langle \hat{\mathbf{O}}_n^m \rangle$  denotes thermal expected values of Stevens operators we defined according to C. Rudowicz [11]. The exchange interactions simulated according to MFA methodology defined by (1) provide simulated properties strongly dependent on only one parameter,  $n_{\text{mol}}$ , which is closely related to the temperature of phase transitions  $T_C$ . It is easy to find the value of  $n_{\text{mol}}$  for correct  $T_C$ , but the value of this parameter can be estimated according to De Gennes scaling [16]:

$$T_C \sim G(f^n), \quad G(f^n) = (g_L - 1)^2 J(J+1) \quad (18)$$

De Gennes scaling is also a useful tool for  $n_{\text{mol}}$  estimation, as charge surroundings can be transferred between ions in series. The CEF part of Hamiltonian contains Stevens CEF parameters  $B_n^m$ . The values of these parameters are only appropriate for the defined ion. The recalculation of  $B_n^m$  parameters defined for an ion A in the crystal lattice surrounding of ion B in the same crystalline position follows the simple scheme:

$$B_n^m(\text{ion A}) \rightarrow A_n^m \rightarrow B_n^m(\text{ion B}) \quad (19)$$

Stevens  $B_n^m$  parameters can be expressed by universal  $A_n^m$  parameters, according to the calculation space used, as follows:

$$|J, J_z\rangle; B_n^m(J, J_z) = \theta_n(J) \langle r_{4f}^n \rangle A_n^m$$

$$|L, S, S_z, L_z\rangle; B_n^m(L, L_z) = \theta_n(L) \langle r_{4f}^n \rangle A_n^m \quad (20)$$

Where values of 2,4,6 –th power of average radius of 4f shell  $\langle r^n \rangle$  have been calculated by many authors using Hartree-Fock-type methodology, and the results can be easily found in the literature. The  $\theta_n$  parameters are the J or L dependent Clebsh-Gordan- type factors, sometimes called  $\alpha, \beta, \gamma$  Stevens factors  $\theta_2=\alpha$ ,  $\theta_4=\beta$ ,  $\theta_6=\gamma$ , which can be expressed by finite equations available in [17,18]. The values of  $\langle r_{4f}^n \rangle$  are stored in the system's open database together with a reference. In all calculations, we used the  $\langle r_{4f}^n \rangle$  values tabulated in [18]. The ability to recalculate CEF parameters between ions and calculation spaces offers a unique chance to establish an acceptable simplification of methodology. The recalculation of CEF parameters in Atomic Matters systems is fully automated, but an explicit Stevens Factors Calculator is also available.

#### 4. Calculation results for DyAl<sub>2</sub>

The CEF parameters used for DyAl<sub>2</sub> were originally estimated by H.G. Purwins and Leson [4] and cited by A. L. Lima et al. [3]. The parameters were provided in cubic Stevens notation:  $B_4 = -(5.5 \pm 1.2) \cdot 10^{-5} \text{ meV}$  and  $B_6 = -(5.6 \pm 0.8) \cdot 10^{-7} \text{ meV}$ . We recalculated the values of Stevens parameters to obtain universal, ion-independent CEF notation  $A_n^m$  according to (19) and (20). The parameters  $A_4 = +7.164 \text{ Ka}_0$  and  $A_6 = -1.038 \text{ Ka}_0$  obtained in this manner define charge surroundings of R ion in a crystal lattice of RAl<sub>2</sub>. A visualization of this potential is shown in figure 2. The triangular shapes that are connected to the location of the coordinating Al ions are located symmetrically in cubic surroundings and reflect the atom position in the elementary cell of Laves phase shown in figure 1.

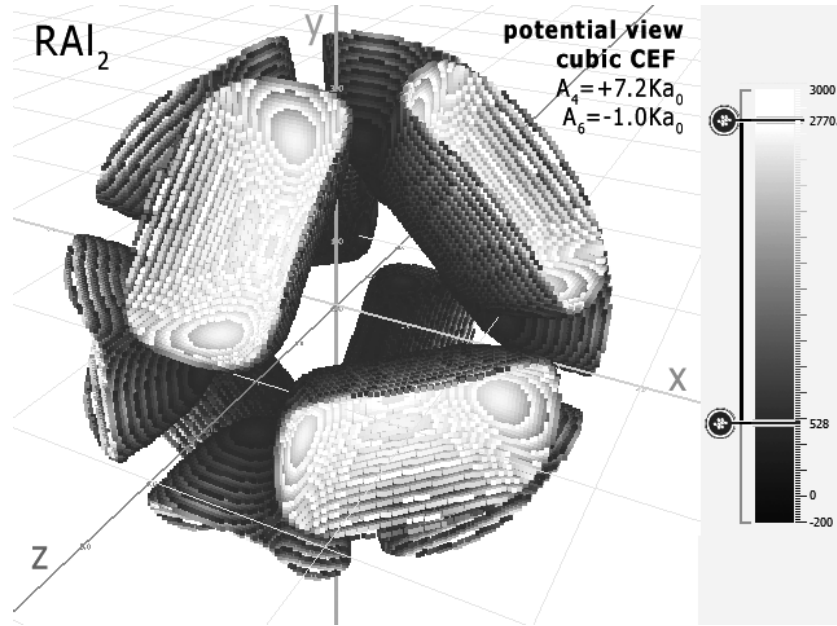


Figure 2. Crystal Field potential visualization of cubic surrounding of R-ions in RAl<sub>2</sub> defined by CEF parameters:  $A_4 = +7.164 \text{ Ka}_0$  and  $A_6 = -1.038 \text{ Ka}_0$ . The visualization of positive sign potential is cut off by the sphere.

The intermetallic compound DyAl<sub>2</sub> has strong magnetocaloric properties at low temperatures. This compound has been extensively studied both theoretically and experimentally [3-6].

In this section, we present the results of an investigation of the magnetic and magnetocaloric properties of a DyAl<sub>2</sub> single crystal. We have attributed the magnetism of DyAl<sub>2</sub> to the Dy ions and calculated the fine electronic structure of the  $4f^9$  electronic system in cubic symmetry taking into account the crystal field and inter-site, spin-dependent exchange interactions. The energy level scheme derived is associated with the reduction of the degeneracy of the lowest atomic term  $^6H$  given by Hund's first two rules.

The full calculated energy level structure in the  $|L, S, L_z, S_z\rangle$  calculation space is shown in figure 3. The obtained overall splitting is strongly dependent on the strength of spin-orbit intra-atomic interactions. We use



the free-ion value of spin orbit constant of  $\text{Ho}^{3+}$  ions  $\lambda = -550\text{K}$  and obtain an overall splitting of  $^6\text{H}$  atomic term of about  $15000\text{K} = 1.3\text{ eV}$ . Details of ground states structure are shown in figure 4.

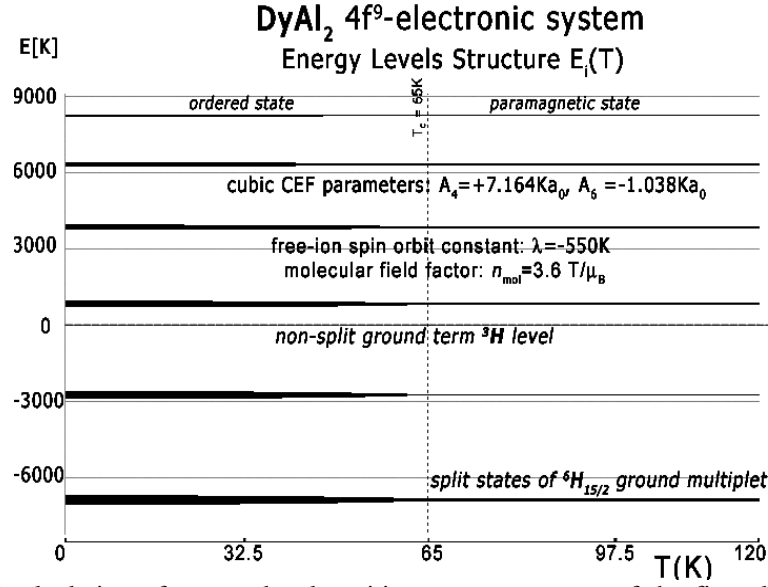


Figure 3. The result of calculation of energy level position vs. temperature of the fine electronic structure of  $4d^9$  electronic configuration of Dy ions in  $\text{DyAl}_2$  in  $|L, S, L_z, S_z\rangle$  space under the influence of intra-atomic spin-orbit coupling, inter-atomic self-consistent molecular magnetic field and Crystal Electric Field (CEF).

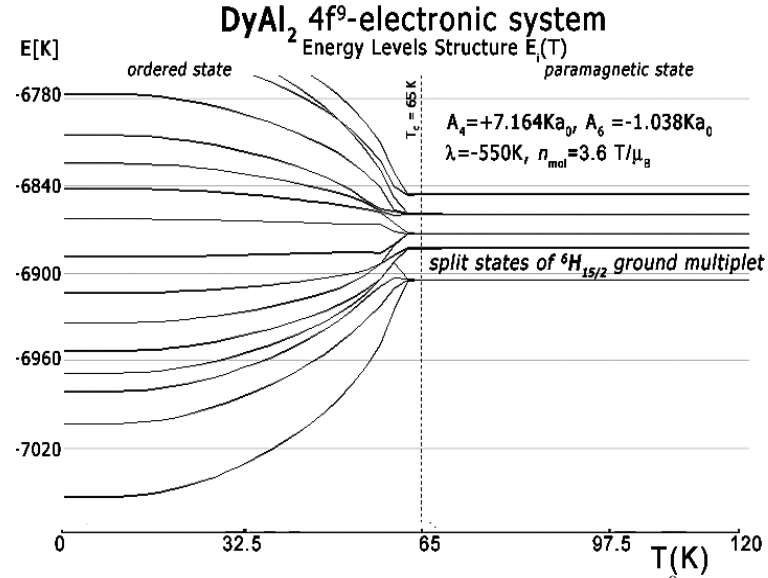


Figure 4. Ground multiplet energy level structure vs. temperature calculated for  $4f^9$  electronic system of Dy ions in  $\text{DyAl}_2$ . At Curie temperature  $T_C = 65\text{K}$ , the structure splits under the influence of molecular field and CEF.

In the absence of an external magnetic field, the induced molecular field splits and moves into degenerated states. The value of the molecular field factor established for  $\text{DyAl}_2$ , which reproduces  $T_C$  well at about  $63\text{K}$ , is  $n_{mol} = 3.6\text{T}/\mu_B$ . Above  $T_C$ , material is in a paramagnetic state and the ground state of Dy ions is degenerated. The ground quartet consists of two quasi doublets. The wave functions of the ground paramagnetic state of Dy ions in  $\text{DyAl}_2$  can be expressed in  $|Jz\rangle$  notation:

$$\begin{aligned}\Gamma_1 &= -0.137|-5.5\rangle + 0.619|-1.5\rangle + 0.723|2.5\rangle - 0.275|6.5\rangle \\ \Gamma_1' &= -0.137|5.5\rangle + 0.619|1.5\rangle + 0.723|-2.5\rangle - 0.275|-6.5\rangle \\ \Gamma_2 &= +0.730|-7.5\rangle - 0.612|-3.5\rangle - 0.303|0.5\rangle - 0.026|4.5\rangle\end{aligned}$$

$$\Gamma_2' = +0.730|7.5\rangle - 0.612|3.5\rangle - 0.303|0.5\rangle - 0.026|-4.5\rangle$$

The molecular field splits these states at  $T < T_C$ . The value of the molecular field changes and at  $T=0$  (absolute zero)  $B_{\text{mol}}=23.6\text{T}$  and its direction is along crystal direction  $[100]$ , which is the x-axis in our CEF potential picture from figure 2. In this condition, the wave function of the ground singlet gets the form:

$$\Gamma_0 = 0.988|-7.5\rangle - 0.153|-3.5\rangle - 0.011|0.5\rangle - 0.0001|4.5\rangle$$

The influence of the external magnetic field applied along different crystal directions for the structure of the lowest electronic states is shown in figure 5 and figure 6. The comparison between the effects of the external magnetic field applied along different directions reveals the appearance of an anomaly in the level structure if an external field is applied along crystal direction  $[110]$ . This anomaly corresponds to the specific heat curve from figure 7, computed in the same external field direction. The specific heat of  $\text{DyAl}_2$  (spec. heat of  $4f^9$  electronic system + Debye crystal lattice component) shown in figure 7 was calculated for the same external field conditions as experimental measurements from [3]. Excellent agreement between calculated specific heat and experimental data is also confirmed if the external magnetic field is applied along direction  $[100]$ . The results of this calculation and reference measurements from [3] are shown in figure 8.

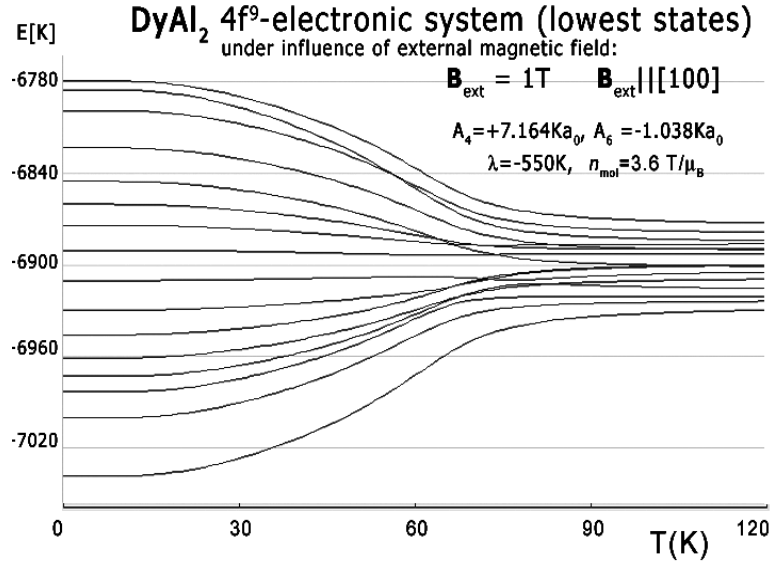


Figure 5. Ground energy level structure vs. temperature calculated for  $4f^9$  electronic system of Dy ions in  $\text{DyAl}_2$  under influence external magnetic field  $B_{\text{ext}}=1\text{T}$  applied along direction  $[100]$ . Parameters of CEF used in calculations and molecular field factor are shown.

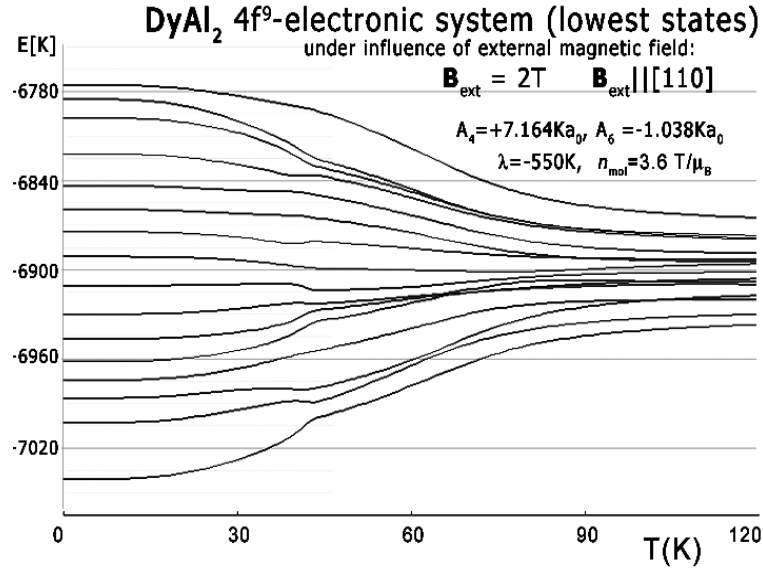


Figure 6. Ground energy level structure vs. temperature calculated for  $4f^9$  electronic system of Dy ions in  $\text{DyAl}_2$  under influence of external magnetic field  $B_{\text{ext}}=2\text{T}$  applied along direction  $[110]$ . Parameters of CEF used in calculations and molecular field factor are shown.

Calculations of electronic structure under the influence of an external magnetic field applied along direction  $[111]$  were also performed. Energy level structure calculated for external magnetic field in this direction does not contain anomalies and is similar to calculations performed for  $B_{\text{ext}}$  along the easy magnetization direction  $[100]$ , as shown in figure 5. Specific heat calculated in these conditions is shown in figure 8.

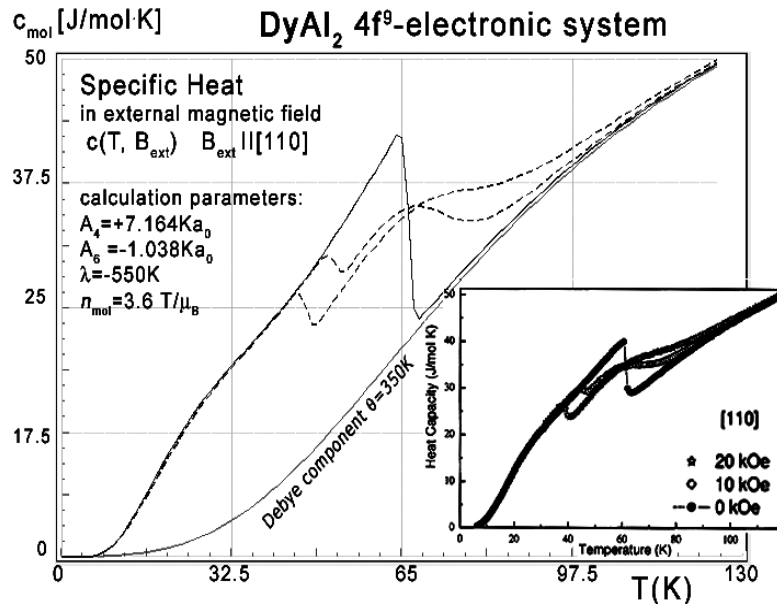


Figure 7. Calculated  $4f$ -electron component of molar specific heat (14) with Debye crystal lattice component ( $\theta=350\text{K}$ ) vs. temperature for Dy ions in  $\text{DyAl}_2$ , under the influence of an external magnetic field applied along direction  $[110]$ . For comparison, the inset shows experimental data from [3] captured in the same external magnetic field conditions as simulated.

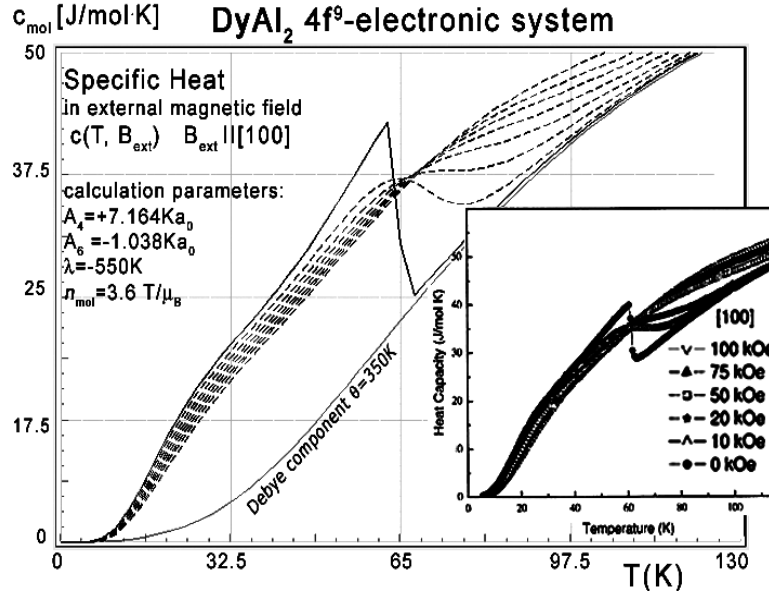


Figure 8. Calculated 4f-electron component of molar specific heat (14) with Debye crystal lattice component ( $\theta=350K$ ) vs. temperature of Dy ions in DyAl<sub>2</sub>, under the influence of an external magnetic field applied along direction [100]. For comparison, the inset shows experimental data from [3] captured in the same external magnetic field conditions as simulated.

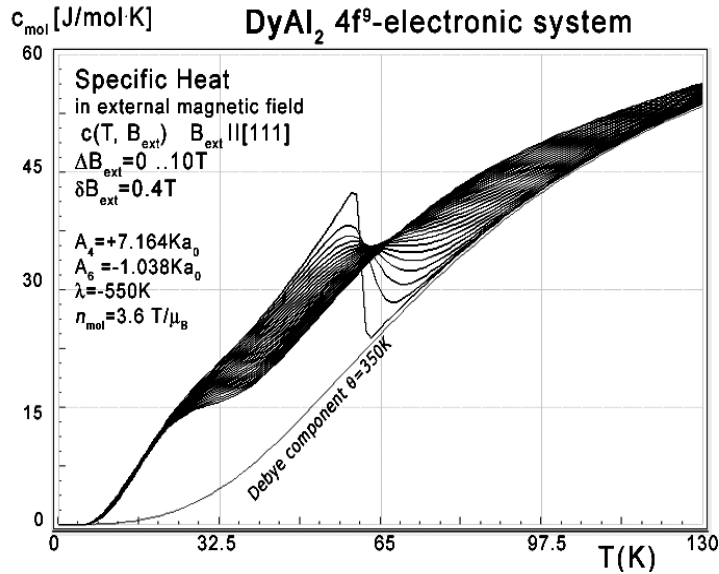


Figure 9. Calculated 4f-electron component of molar specific heat (14) with Debye crystal lattice component ( $\theta=350K$ ) vs. temperature of Dy ions in DyAl<sub>2</sub>, under the influence of an external magnetic field  $B_{\text{ext}}$  from 0 to 10T applied along direction [111].

Collected data of specific heat makes it possible to calculate isothermal entropy change  $-\Delta S(T, B_{\text{ext}})$  according to (16), the same methodology as used by experimentalist [3-7]. Isothermal entropy change calculated with various external magnetic fields applied along all main directions of cubic structure is presented in figures 10, 11 and 12. The reference data taken from experimental measurement [3] is shown in the insets.

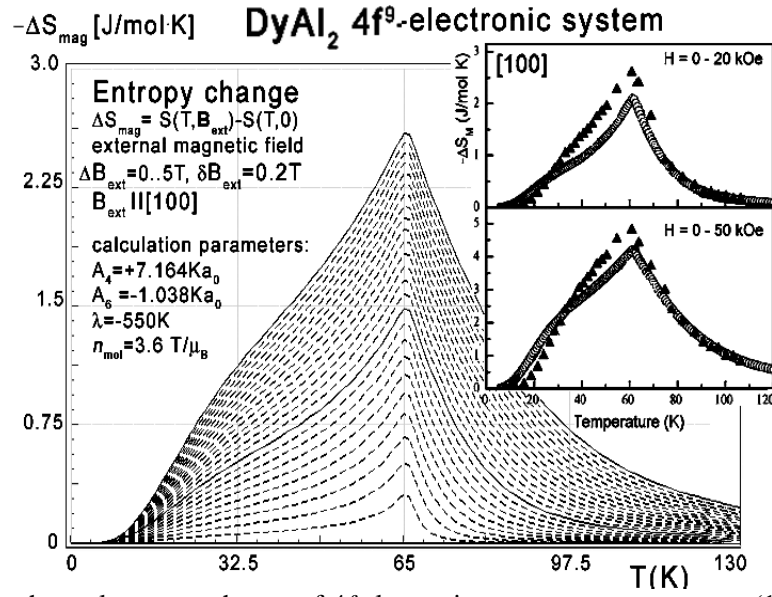


Figure 10. Calculated isothermal entropy change of 4f-electronic system vs. temperature (16) of Dy ions in DyAl<sub>2</sub>, under the influence of various values of external magnetic field from 0 to 5 T, with step 0.2 T applied along direction [100]. Inset: isothermal entropy change obtained from experimental data; black triangles -extracted from the magnetization, circles - extracted from specific heat, for the DyAl<sub>2</sub> single crystal aligned along the same direction, taken from [3]. The solid lines are congruent with the experimental data calculated for the  $B_{\text{ext}}=2 \text{ T}$  and  $B_{\text{ext}}=5 \text{ T}$ .

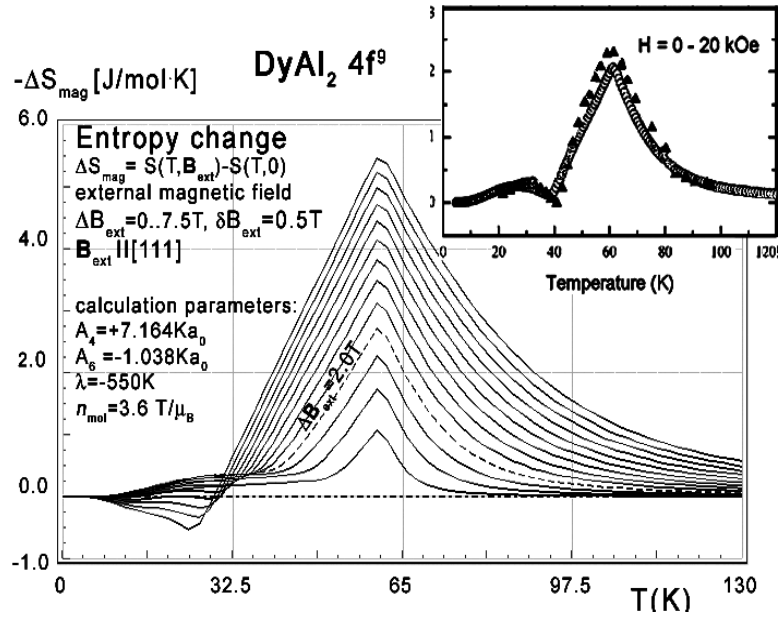


Figure 11. Calculated isothermal entropy change vs. temperature (16) for various values of external magnetic fields from 0 to 2 T with step 0.1 T, applied along direction [110] of DyAl<sub>2</sub> crystal lattice. Inset: black triangles show isothermal entropy change obtained from experimental data extracted from the magnetization; empty circles show specific heat for a DyAl<sub>2</sub> single crystal aligned along the same direction, taken from [3].

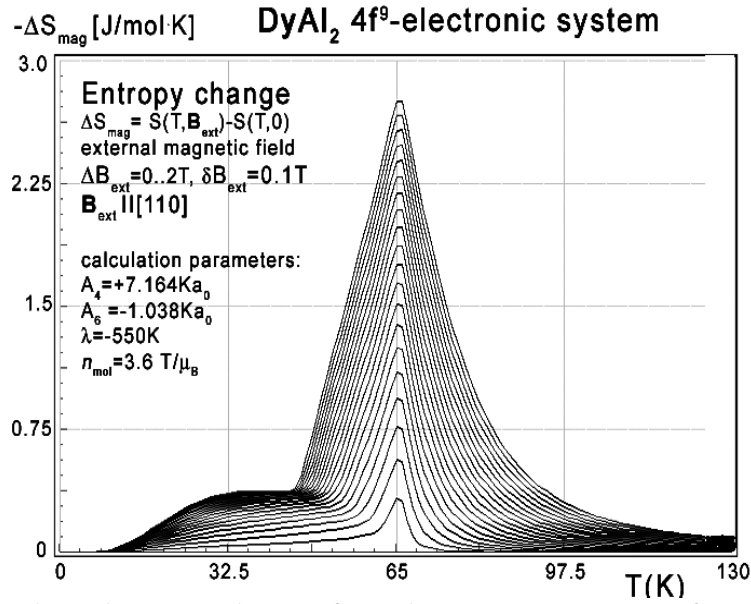


Figure 12. Calculated isothermal entropy change of  $\text{DyAl}_2$  vs. temperature (16) for various values of external magnetic field from 0 to 2T with step 0.1T, applied along diagonal direction [110].

The anisotropic behavior of calculated thermomagnetic properties is reflected in the magnetocrystalline anisotropy constant calculations. The results of  $K_i(T)$  calculations according to (17) in the absence of external magnetic field are shown in figure 13.

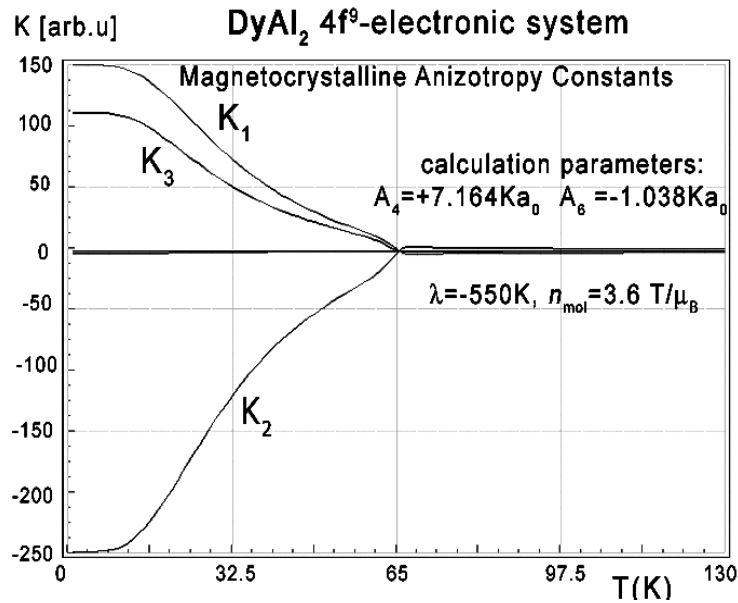


Figure 13. Calculated according to (17), magnetocrystalline anisotropy constants  $K_1, K_2$  and  $K_3$  vs. temperature, calculated for Dy ions in  $\text{DyAl}_2$  under the influence of CEF and molecular magnetic field.

For completeness, magnetic moment calculations vs. temperature under various external magnetic field conditions were performed. The results of  $\mathbf{m}(T, \mathbf{B}_{\text{ext}})$  are presented in figures 14, 15 and 16. Figure 14 clearly confirms direction [100] as an easy magnetization axis. The applied external magnetic field along this direction confirms perfect parallel directions of magnetic vector and external magnetic field (note: in cubic symmetry  $[100]=[010]=[001]$ ).

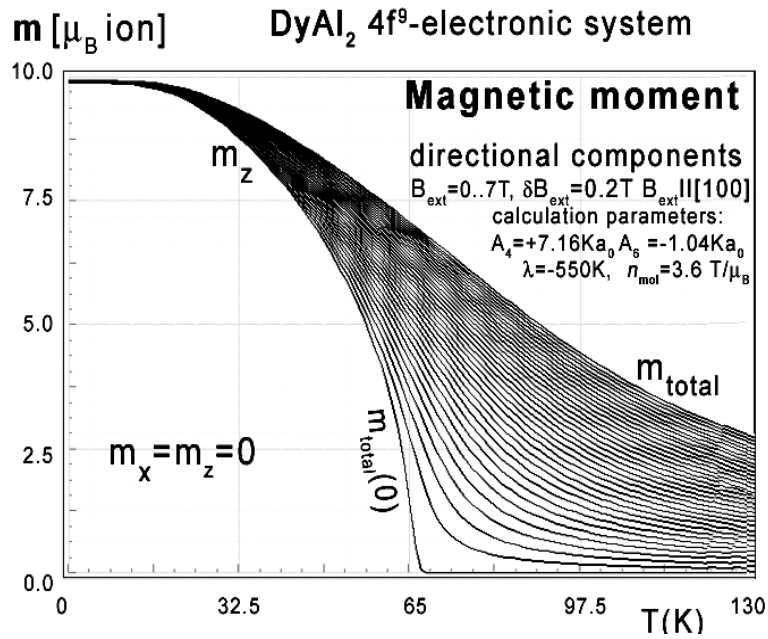


Figure 14. Calculated x,y,z-directional components of total magnetic moment vs. temperature, calculated for Dy ions in DyAl<sub>2</sub> under influence of CEF and molecular magnetic field and various values of external magnetic field from 0 to 7T with step 0.2T applied along direction [100].

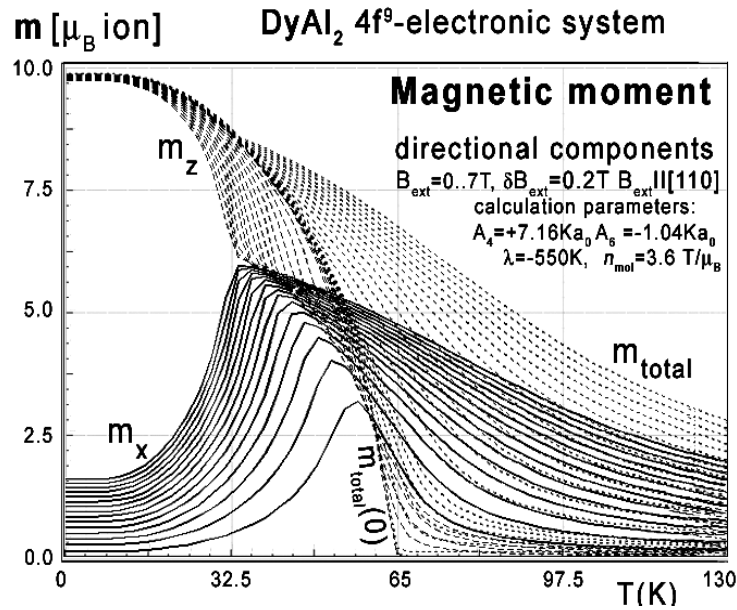


Figure 15. Calculated x components (solid lines), z-components (dashed lines) of total magnetic moment  $m_{\text{total}}$  (dotted lines) vs. temperature, calculated for Dy ions in DyAl<sub>2</sub> under influence of CEF, molecular magnetic field, and various values of external magnetic field from 0 to 7T with step 0.2T applied along direction [110].

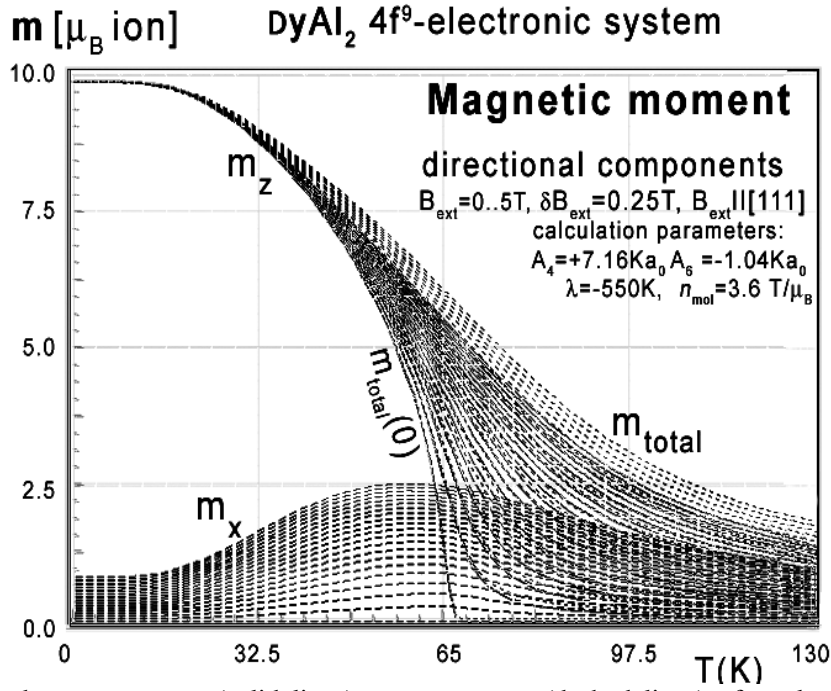


Figure 16. Calculated x components (solid lines), z-components (dashed lines) of total magnetic moment  $m_{\text{total}}$  (dotted lines) vs. temperature, calculated for Dy ions in  $\text{DyAl}_2$  under influence of CEF, molecular magnetic field, and various values of external magnetic field from 0 to 7T with step 0.2T applied along direction [111]. Magnetic moment calculated in an external magnetic field parallel to direction [110] reveals unusual behavior of the directional component of the total moment. Similar behavior of magnetic moment directions was reported in [3-5].

##### 5. Calculation results for $\text{HoAl}_2$ and $\text{ErAl}_2$

Here, we present the results of an investigation of the magnetic and magnetocaloric properties of a  $\text{HoAl}_2$  and  $\text{ErAl}_2$  single crystal. The predictions of properties are completely achieved without free parameters. We use established cubic CEF for  $\text{DyAl}_2$  parameters in Stevens notation from [4] and recalculated them for  $\text{Ho}^{3+}$  and  $\text{Er}^{3+}$  ions.

As above, we attributed the magnetism of  $\text{HoAl}_2$  and  $\text{ErAl}_2$  and the magnetism of  $\text{HoAl}_2$  to the Ho ions and performed calculations of the fine electronic structure of the  $4f^{10}$  and  $4f^{11}$  electronic systems, respectively. All calculations was performed for cubic symmetry, taking into account the crystal field and inter-site, spin-dependent exchange interactions. The energy level scheme derived is associated with the reduction of the degeneracy of the lowest atomic term ( $^5\text{I}$  and  $^4\text{I}$  for Ho and Er ions, respectively) given by Hund's first two rules. The value of molecular field factor  $n_{\text{mol}}$  for  $\text{HoAl}_2$  and  $\text{ErAl}_2$  was established according to  $n_{\text{mol}}^{\text{Dy}} = 3.6\text{T}/\mu_{\text{B}}$  for  $\text{DyAl}_2$  and de Gennes scaling (18) [11]. The comparison between experimentally found Curie temperature  $T_{\text{C}}$  and de Gennes scaling is shown in figure 17.



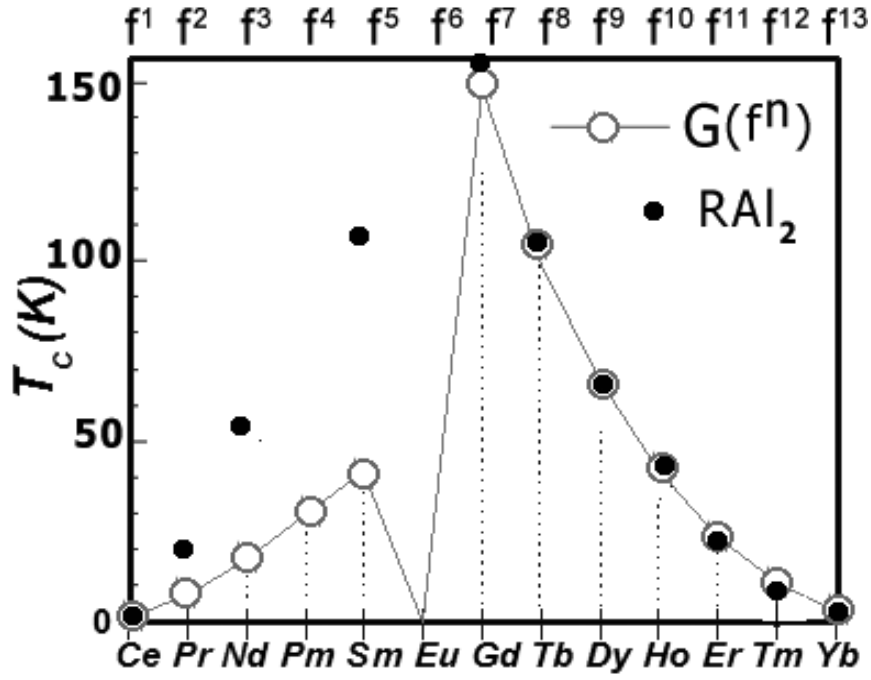


Figure 17. De Gennes scaling of Curie temperature  $T_C$  for all rare-earth ions in series  $RAl_2$  in comparison to experimental data from [4].

Experimental values of  $T_C$  for  $RAl_2$  compounds [3-7] and the theory are in good agreement for ‘heavy Rare Earths’ elements from Gd ( $4f^7$ ) to Yb ( $4f^{13}$ ). De Gennes relations [10,14] makes it possible to establish molecular field factor for  $HoAl_2$   $n_{mol}^{Ho}=2.1T/\mu_B$  and for  $ErAl_2$   $n_{mol}^{Er}=0.95T/\mu_B$ .

### 5.1. Calculated properties of $HoAl_2$ single crystals

The electronic configuration of  $_{67}Ho$  atoms consists of a closed shell inactive atomic core [ $_{54}Xe$ ], electronic system  $4f^{10}$  and ‘outer electrons  $5d^16s^2$ . We attributed the magnetic properties of  $HoAl_2$  compound as an effect of properties of  $4f^{10}$  electronic system under influence of electromagnetic interactions defined according to the description in the theory section. The starting point of our analysis is the ground atomic term  $^5I$  with quantum number of orbital angular momentum  $L=6$  and total spin  $S=2$ .

The full calculated energy level structure in  $|L,S,L_z,S_z\rangle$  calculation space is shown in figure 18. The obtained overall splitting is strongly dependent on the strength of spin-orbit intra-atomic interactions. We used free-ion value of spin orbit constant of  $Ho^{3+}$  ions  $\lambda=-780K$  [17] and obtained overall splitting of  $^2F$  atomic term at about  $20350K = 1.753 eV$ .

Details of ground states structure are shown in figure 18.

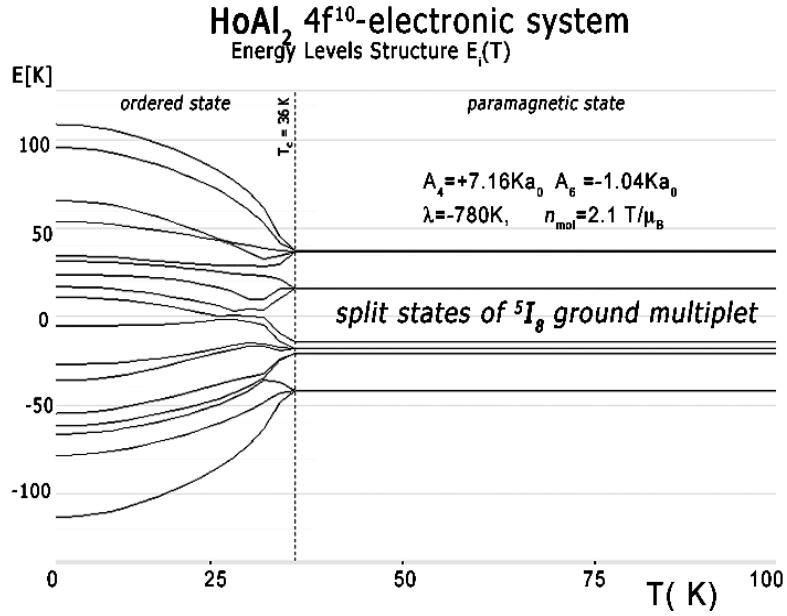


Figure 18. The result of calculation of ground multiplet energy levels structure vs. temperature calculated vs. temperature of the fine electronic structure of  $4f^{10}$  electronic configuration of Ho ions in HoAl<sub>2</sub> in  $|L, S, L_z, S_z\rangle$ . At Curie temperature  $T_C = 36 \text{ K}$  structure splits under the influence of molecular field.

In the absence of an external magnetic field, the induced molecular field splits and moves into degenerated states. The value of the molecular field factor established for HoAl<sub>2</sub> which reproduce  $T_C$  well at about 36 K is  $n_{mol} = 2.1 \text{ T}/\mu_B$ .

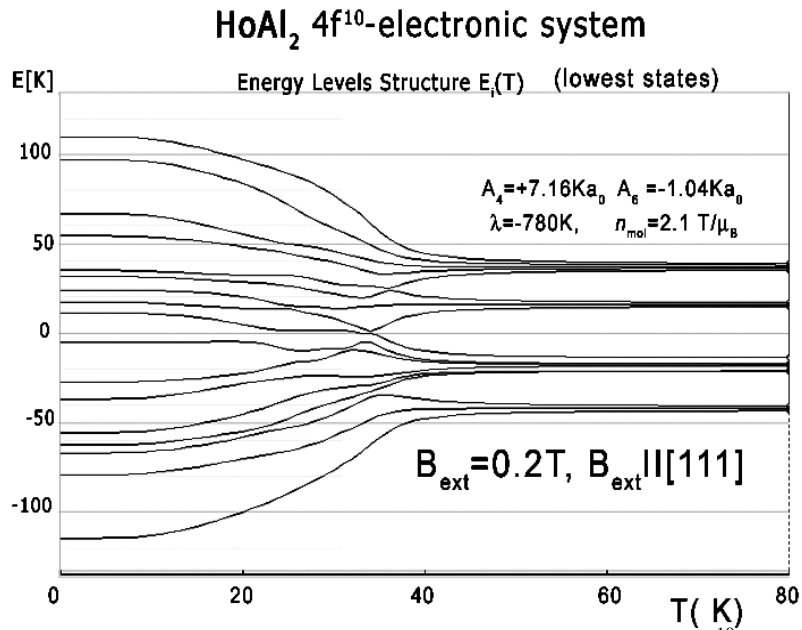


Figure 19. Ground multiplet energy levels structure vs. temperature calculated for  $4f^{10}$  electronic system of Ho ions in HoAl<sub>2</sub> under the influence of a small external magnetic field of 0.2 T applied along crystal direction [111].

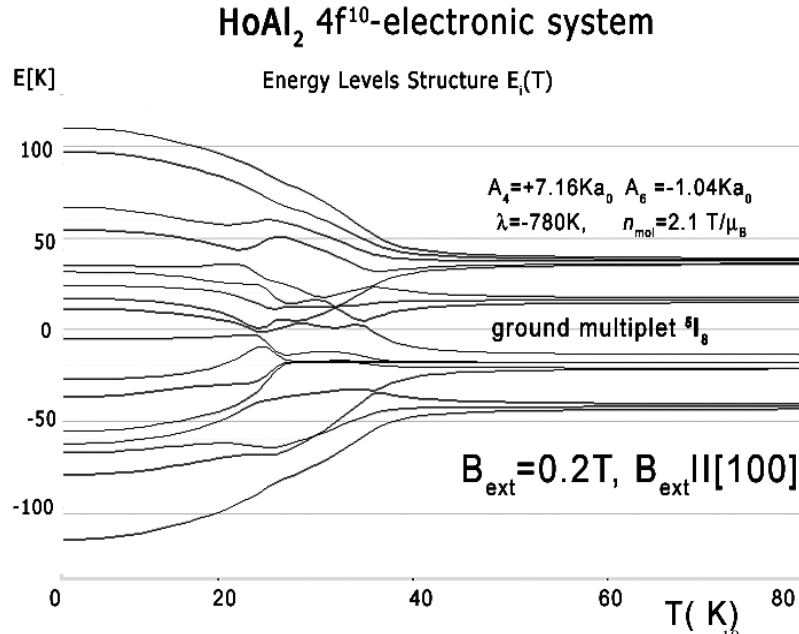


Figure 20. Ground multiplet energy levels structure vs. temperature calculated for 4f<sup>10</sup> electronic system of Ho ions in HoAl<sub>2</sub> under the influence of a small external magnetic field of 0.2T applied along crystal direction [111].

Above  $T_C$ , in a paramagnetic state, the ground state is degenerated and consist of 3 states. The ground triplet wave functions of ground state of Ho ions (4f<sup>10</sup> electronic system) in HoAl<sub>2</sub> in a paramagnetic state can be expressed in  $|Jz\rangle$  notation as:

$$\begin{aligned}\Gamma_1 &= +0.4|-6\rangle + 0.583|-2\rangle - 0.583|+2\rangle - 0.4|+6\rangle \\ \Gamma_2 &= -0.086|-5\rangle - 0.367|-1\rangle + 0.5807|+3\rangle + 0.72|+7\rangle \\ \Gamma_3 &= -0.086|+5\rangle - 0.367|+1\rangle + 0.581|-3\rangle + 0.722|-7\rangle\end{aligned}$$

A molecular field split these states at  $T < T_C$ . The value of the molecular field changes, and at  $T=0$  (absolute zero)  $B_{mol}=13T$  and its direction is along crystal direction [110]. In this condition, the wave function of a ground singlet gets the form:

$$\Gamma_0 = -0.291|-8\rangle + 0.588|-7\rangle - 0.410|-6\rangle + 0.223|-5\rangle - 0.257|-4\rangle + 0.38|-3\rangle - 0.312|-2\rangle + 0.151|-1\rangle - 0.014|0\rangle - 0.081|+1\rangle + 0.09|+2\rangle - 0.040|+3\rangle + 0.010|+4\rangle - 0.011|+5\rangle + 0.018|+6\rangle - 0.012|+7\rangle + 0.002|+8\rangle$$

The electronic structure obtained in the absence of an external magnetic field is fragile; even a small magnetic field applied along direction [100] or [111] forces the structure to change the order of states and creates an anomaly at low temperatures. The influence of a small external magnetic field applied along direction [111] for the structure of the lowest electronic states is shown in figure 20. The position of this anomaly corresponds with peaks on specific heat curves. The calculated specific heat for a HoAl<sub>2</sub> single crystal under the influence of an external magnetic field applied along various crystal directions is presented in figures 21, 22 and 23.

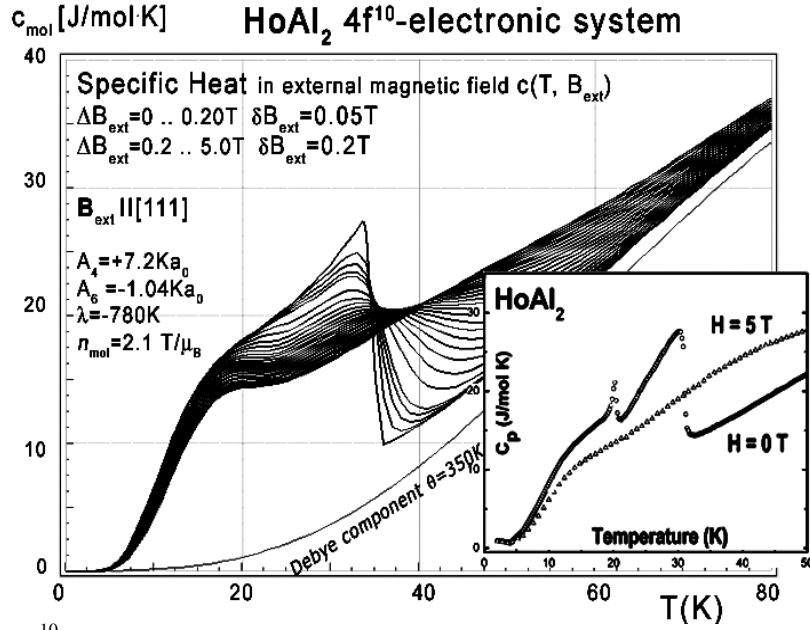


Figure 21. Calculated  $4f^{10}$ -electronic system component of molar specific heat (14) with Debye crystal lattice component ( $\theta=350\text{K}$ ) vs. temperature for Ho ions in  $\text{HoAl}_2$ , under the influence of an external magnetic field applied along direction [100]. Inset: experimental data from [7].

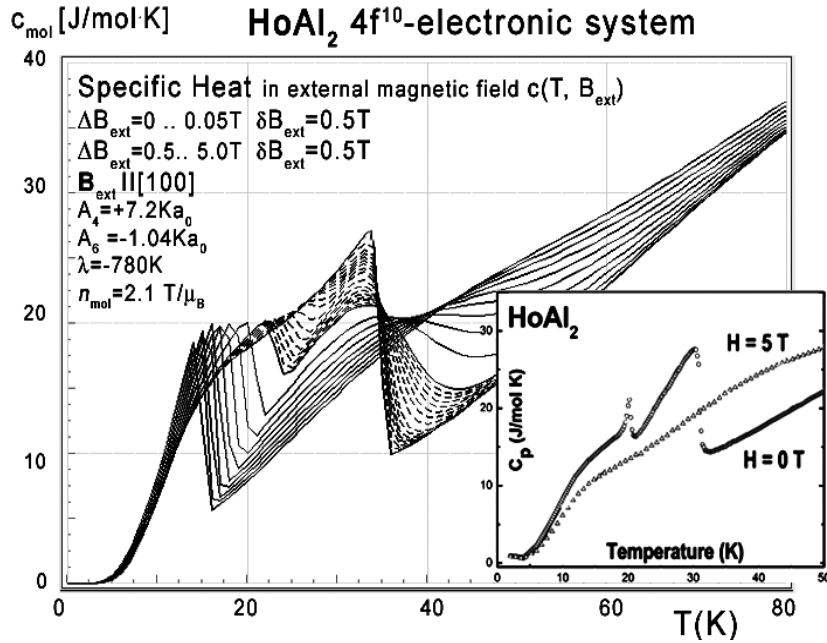


Figure 22. Calculated molar specific heat (14) vs. temperature for Ho ions in  $\text{HoAl}_2$ , under the influence of an external magnetic field applied along [100] direction. Inset: experimental data from [7].

The closer look at the unusual behaviour of the  $4f$ -electron component of specific heat simulated under the influence of an external magnetic field along ‘diagonal’ direction [111] is shown in figure 23.

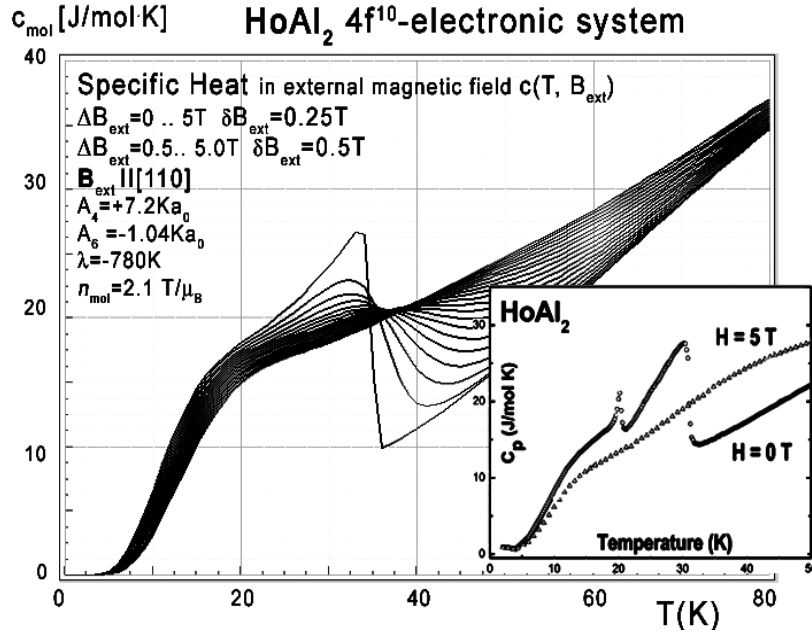


Figure 23. Calculated molar specific heat (14) vs. temperature for Ho ions in HoAl<sub>2</sub>, under the influence of an external magnetic field applied along easy magnetization axis, direction [100]. Inset: experimental data from [7].

We have not found comparative experimental data for specific heat measurements, but F. W. Wang [19] provides data of measured specific heat change  $\Delta c(T, B_{ext})$  defined as:

$$\Delta c(T, B_{ext}) = c(T, B_{ext}) - c(T, 0) \quad (21)$$

for measurements for  $\Delta B_{ext} = 5T$ . Comparison between data from [8] and our simulations of  $\Delta c(T, B_{ext})$  is shown in figure 25. The simulation for  $\Delta B_{ext} = 5T$  in this figure is represented by a solid line.

Collected data of specific heat makes it possible to calculate isothermal entropy change  $-\Delta S(T, B_{ext})$  according to (16), the same methodology as used by experimentalist [3-7]. Isothermal entropy changes calculated with various external magnetic fields applied along all main directions of the/a cubic structure are presented in figure 24, 25 and 26.

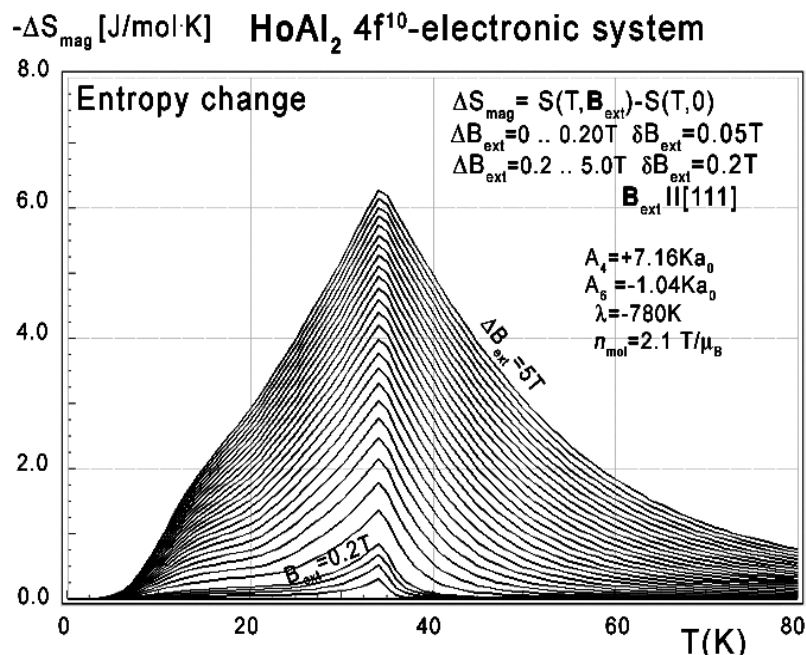


Figure 24. Calculated isothermal entropy change of  $4f^{10}$ -electronic system vs. temperature (16) of Ho ions in  $\text{HoAl}_2$ , under the influence of various external magnetic field values from 0 to 0.2T, with step 0.05T and from 0 to 0.2 to 5.0T, with step 0.2T applied along direction [111].

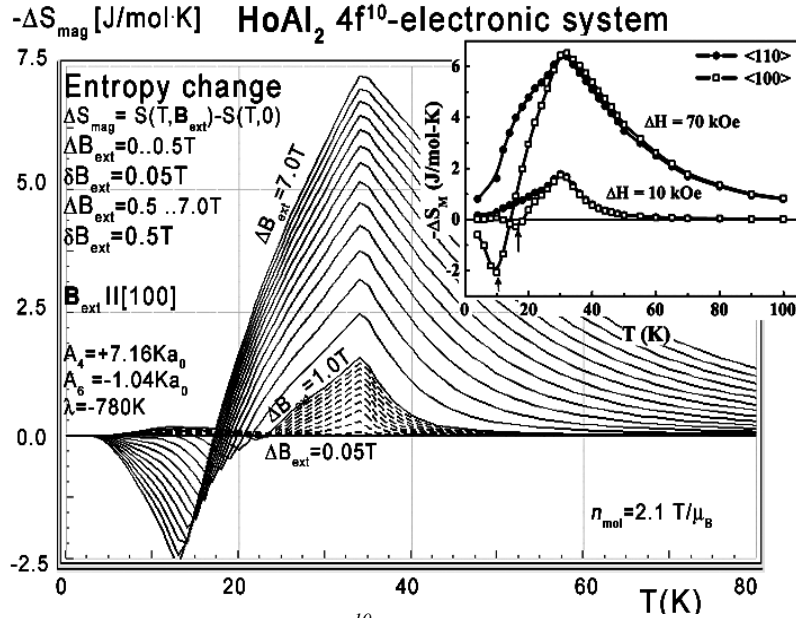


Figure 25. Calculated isothermal entropy change of  $4f^{10}$ -electronic system vs. temperature (16) of Ho ions in  $\text{HoAl}_2$ , under the influence of various external magnetic field values from 0 to 0.5T, with step 0.05T and from 0 to 0.5 to 7.0T, with step 0.5T applied along direction [100]. Inset: experimental data from [8].

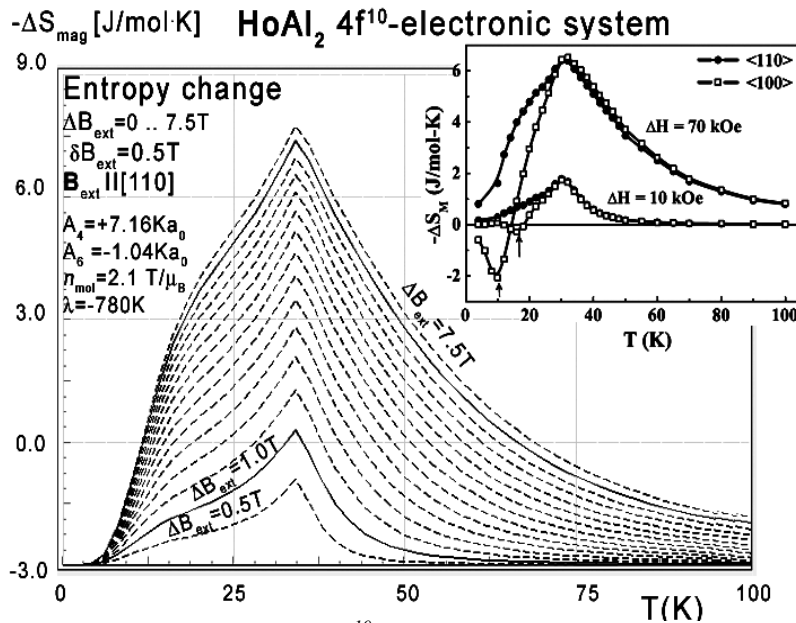


Figure 26. Calculated isothermal entropy change of  $4f^{10}$ -electronic system vs. temperature (16) of Ho ions in  $\text{HoAl}_2$ , under the influence of various external magnetic field values from 0 to 7.5T, with step 0.5T applied along direction [111]. Inset: experimental data from [8].

The anisotropic behavior of calculated thermomagnetic properties is reflected in magnetocrystalline anisotropy constant calculations. The results of  $K_i(T)$  calculations according to (17) in the absence of an external magnetic field are shown in figure 27.

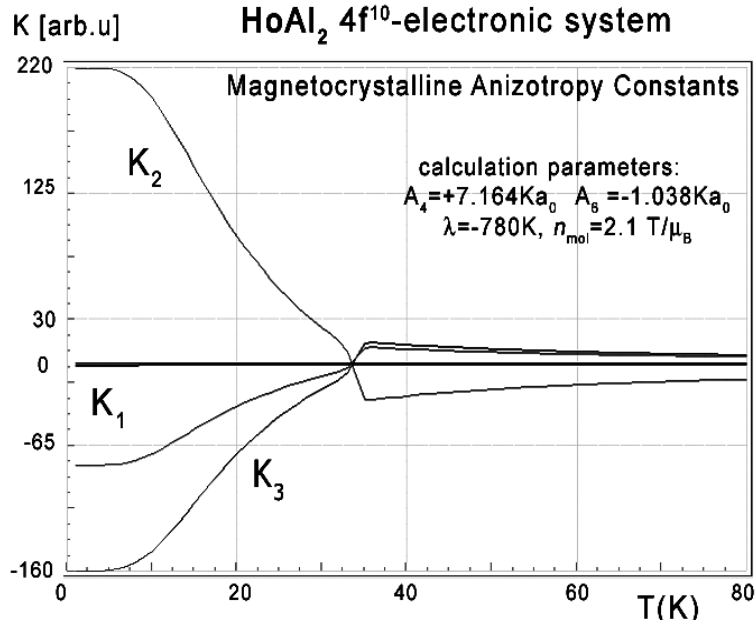


Figure 27. Calculated according to (17) magnetocrystalline anisotropy constants  $K_1, K_2$  and  $K_3$  vs. temperature, calculated for Ho ions in  $\text{HoAl}_2$  in absence of external magnetic field.

The results of  $K_i(T)$  calculations according to (17) under the influence of external magnetic field  $B_{\text{ext}}=1\text{T}$  applied along direction [100] are shown in figure 28.

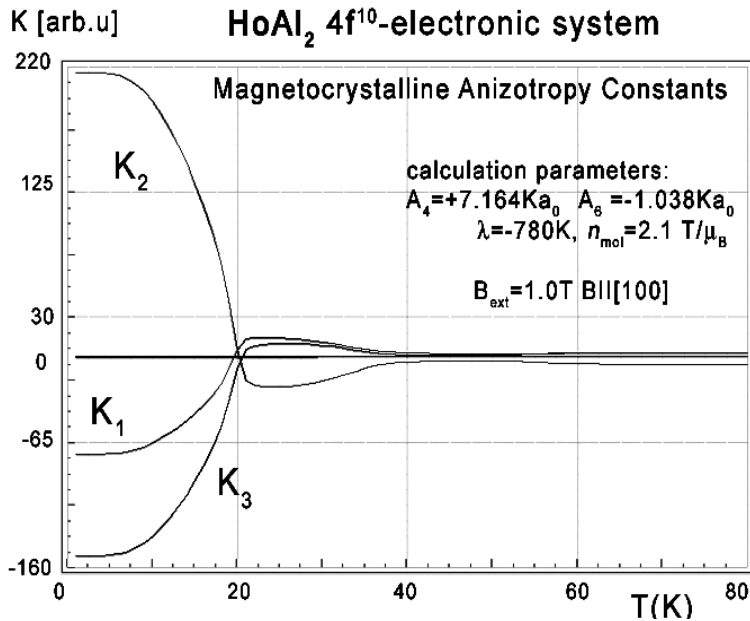


Figure 28. Calculated according (17) magnetocrystalline anisotropy constants  $K_1, K_2$  and  $K_3$  vs. temperature, calculated for Ho ions in  $\text{HoAl}_2$  under influence of CEF and molecular magnetic field.

For completeness, magnetic moment calculations vs. temperature under various external magnetic field conditions were performed. The results of  $\mathbf{m}(T, \mathbf{B}_{\text{ext}})$  are presented in figures 29, 30 and 31. The simulated thermal evolution of magnetic moment components under the influence of external magnetic field along direction [110] shown in figure 30 clearly confirms direction [110] as an easy magnetization axis of  $\text{HoAl}_2$  in the lowest temperatures. The applied external magnetic field along this direction confirms perfect parallel directions of magnetic vector and induced external magnetic field.

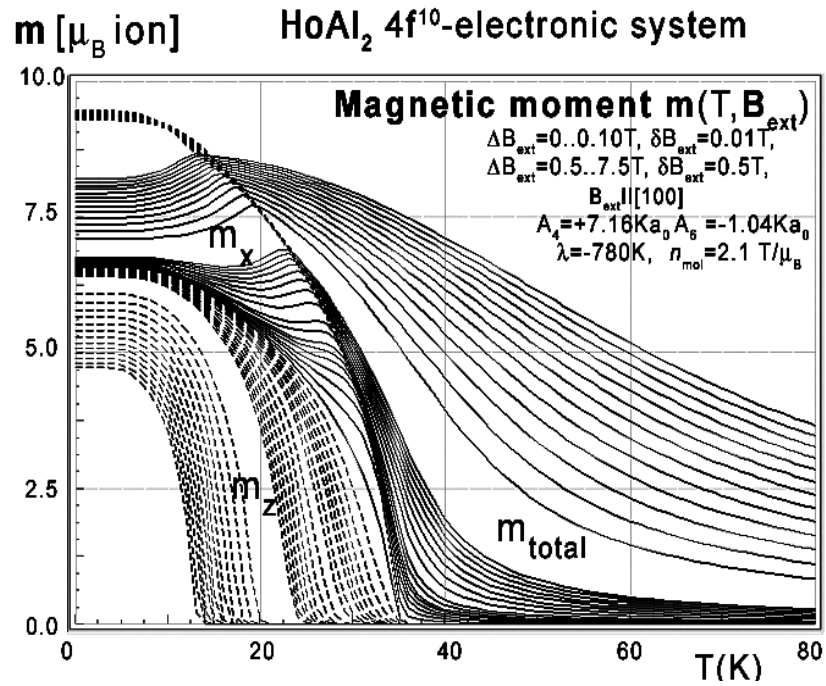


Figure 29. Calculated x,y,z-directional components of total magnetic moment vs. temperature, calculated for Ho ions in HoAl<sub>2</sub> the influence of various external magnetic field values from 0 to 0.1T, with step 0.01T and from 0.5 to 7.5T with step 0.5T applied along direction [100].

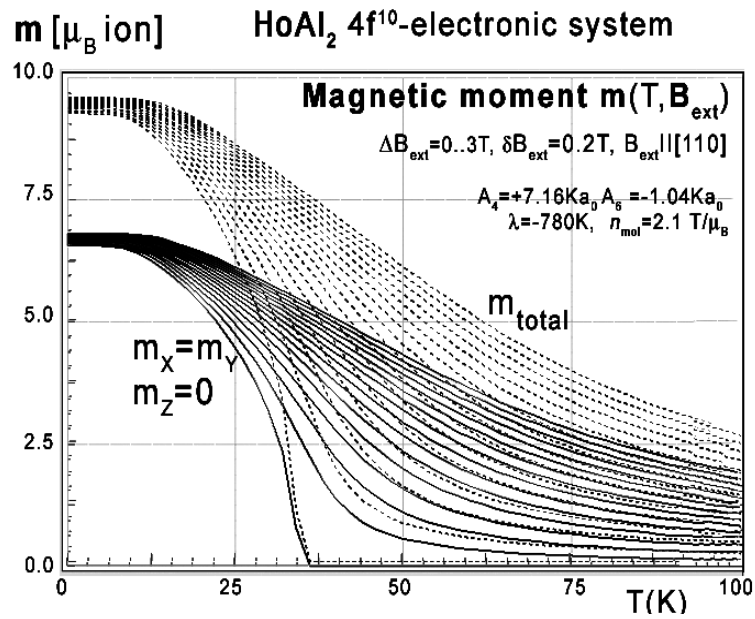


Figure 30. Calculated x - components (solid lines), z-components (dashed lines) of total magnetic moment  $m_{\text{total}}$  (dotted lines) vs. temperature, calculated for Ho ions in HoAl<sub>2</sub> under influence of CEF, molecular magnetic field and various values of external magnetic field from 0 to 3T with step 0.2T applied along direction [110].



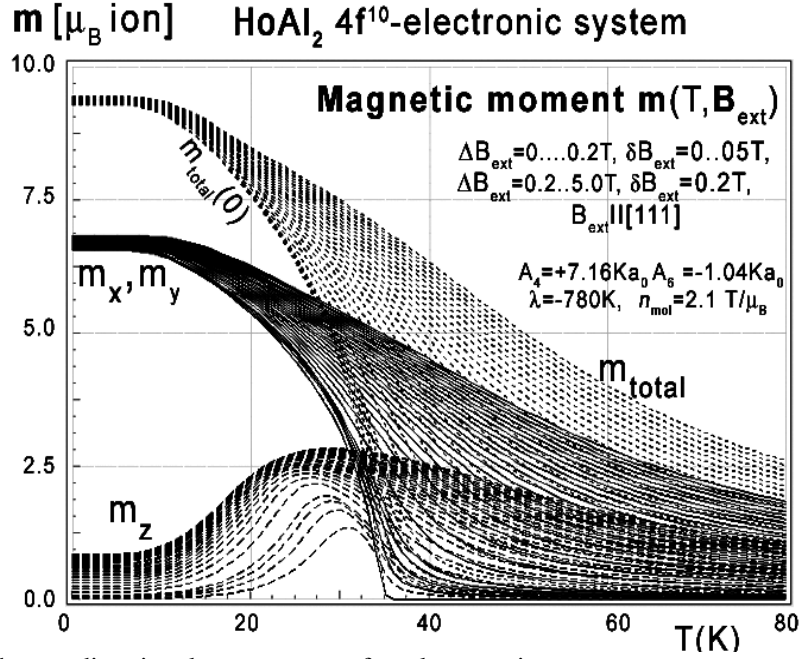


Figure 31. Calculated x,y,z-directional components of total magnetic moment vs. temperature, calculated for Ho ions in  $\text{HoAl}_2$  under influence of CEF and molecular magnetic field and various values of external magnetic field from 0 to 0.2T, with step 0.05T and from 0.2 to 5.0T with step 0.2T applied along direction [111].

Magnetic moment calculated in external magnetic field parallel to [111] and [100] direction reveals unusual behavior of the directional component of total moment. Similar behavior of magnetic moment directions was reported in [20], but most of the presented results of calculations of properties of  $\text{HoAl}_2$  still await experimental verification.

We found only a few reports about measurements of thermomagnetic properties of  $\text{HoAl}_2$  single crystals. Some experimental comparative data of isothermal entropy change measured on  $\text{HoAl}_2$  single crystals is provided by L.A. Gil et al. [7], and interesting entropy change is provided by M. Patra et al. [8]. All experimental data from [4,5] confirms the correctness of our approach in thermomagnetic properties calculations of  $\text{HoAl}_2$ .

## 5.2. Calculation results for $\text{ErAl}_2$ single crystals

The electronic configuration of Er atoms consists of a closed shell inactive atomic core  $[\text{Xe}]$ , electronic system  $4f^{11}$  and ‘outer electrons’  $5d^1 6s^2$ . We attribute the magnetic properties of  $\text{ErAl}_2$  compound to be an effect of properties of  $4f^{11}$  electronic system under the influence of electromagnetic interactions defined according to the description in the theory section. The starting point of our analysis is the ground atomic term  $^4\text{I}$  with quantum number of orbital angular momentum  $L=6$  and total spin  $S=3/2$ .

The full calculated energy level structure in  $|L, S, L_z, S_z\rangle$  calculation space reveals good separation of ground multiplet  $^4\text{I}_{15/2}$  states from the rest of eigenstates of the fine electronic structure. The overall energy levels splitting is strongly dependent on the strength of spin-orbit intra-atomic interactions. We used free-ion value of spin orbit constant of  $\text{Er}^{3+}$  ions  $\lambda = -1170\text{K}$  [17] and obtained overall splitting of  $^4\text{I}$  atomic term at about  $22900\text{K} = 1.97\text{ eV}$ . Details of ground multiplet  $^4\text{I}_{15/2}$  states structure are shown in figure 32.

In the absence of an external magnetic field, the induced molecular field at  $T < T_C$  splits degenerated states. The value of the molecular field factor established according to de Gennes scaling [16] for  $\text{ErAl}_2$  which reproduce  $T_C$  well at about 11K is  $n_{\text{mol}} = 0.95\text{T}/\mu_B$ . Above  $T_C$ , in a paramagnetic state, the ground state is degenerated. The ground quartet consists of two quasi doublets. The wave functions of ground state of Er ( $4f^{11}$  electronic system) ions in  $\text{ErAl}_2$  in a paramagnetic state can be expressed in  $|Jz\rangle$  notation as:

$$\begin{aligned}\Gamma_1 &= -0.44|-6.5\rangle + 0.72|-2.5\rangle + 0.458|1.5\rangle - 0.29|5.5\rangle \\ \Gamma_1^* &= -0.44|+6.5\rangle + 0.72|+2.5\rangle + 0.458|-1.5\rangle - 0.28|-5.5\rangle \\ \Gamma_2 &= -0.61|-7.5\rangle + 0.78|-3.5\rangle + 0.143|+0.5\rangle - 0.04|+4.5\rangle \\ \Gamma_2^* &= 0.61|+7.5\rangle + 0.781|+3.5\rangle + 0.14|-0.5\rangle + 0.04|-4.5\rangle\end{aligned}$$

A molecular field split these states at  $T < T_C$ . The value of the molecular field changes, and at  $T=0$  (absolute zero)  $B_{\text{mol}}=4.46\text{T}$  and its direction is along crystal direction  $[110]$ . In this condition, the wave function of a ground singlet gets the form:

$$\Gamma_0 = -0.483|-7.5\rangle + 0.32|-6.5\rangle - 0.111|-5.5\rangle - 0.12|-4.5\rangle + 0.577|-3.5\rangle - 0.459|-2.5\rangle + 0.159|-1.5\rangle - 0.029|-0.5\rangle + 0.104|+0.5\rangle - 0.185|+1.5\rangle + 0.116|+2.5\rangle - 0.03|+3.5\rangle - 0.017|+4.5\rangle + 0.066|+5.5\rangle - 0.048|+6.5\rangle + 0.015|+7.5\rangle$$

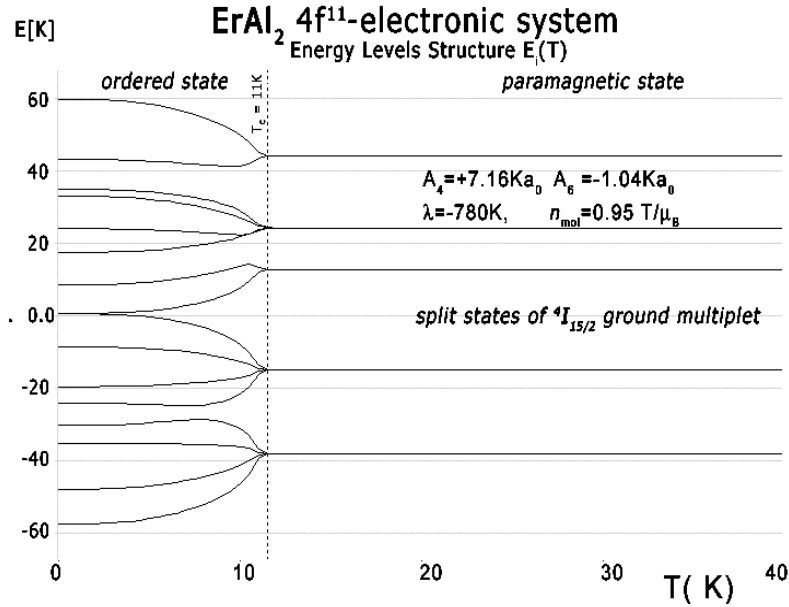


Figure 32. The result of calculation of energy level positions vs. temperature of the fine electronic structure of  $4f^{11}$  electronic configuration of Er ions in  $\text{ErAl}_2$

The structure of states is sensitive on external magnetic field influence. The effect of an external magnetic field  $B_{\text{ext}}=1\text{T}$  applied along direction  $[111]$  for the structure of the lowest electronic states is shown in figure 33.

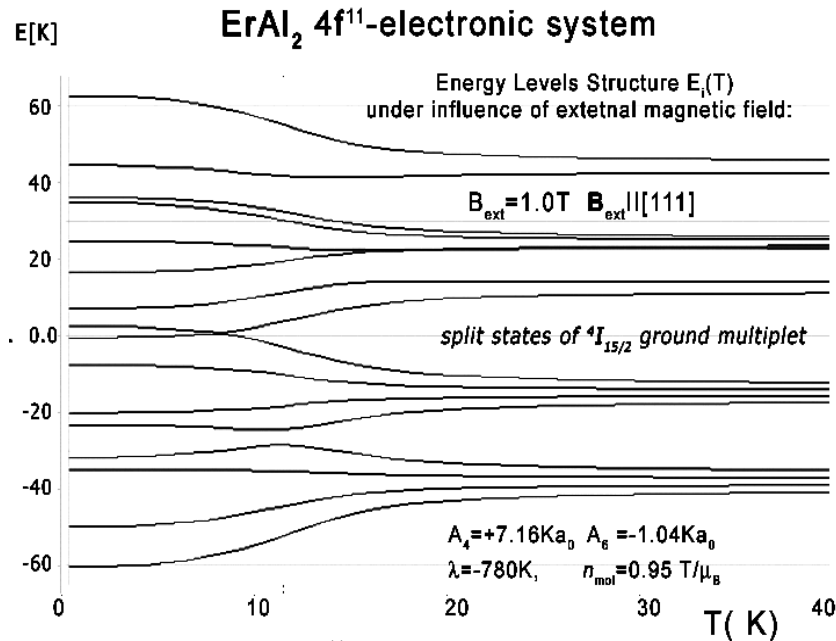


Figure 33. Calculated energy level structure of  $4f^{11}$  electronic system of Er ions vs. temperature under the influence of external magnetic field  $B_{\text{ext}}=1\text{T}$  applied along direction  $[111]$ .

The energy level structure makes it possible to calculate the  $4f$ -electron component of specific heat. The result of calculation of specific heat under the influence of an external magnetic field compared to experimental data from [21] is shown in figures 34.35 and 36.

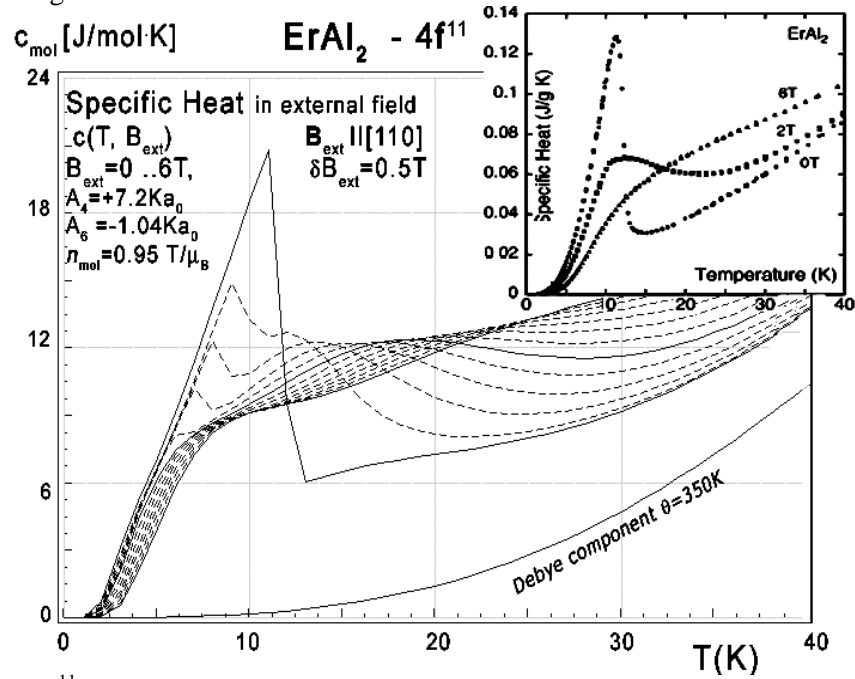


Figure 34. Calculated  $4f^{11}$ -electronic system component of molar specific heat (14) with Debye crystal lattice component ( $\theta=350\text{K}$ ) vs. temperature of Er ions in  $\text{ErAl}_2$ , under the influence of external magnetic field from 0 to 6T with step 0.2T. Inset: experimental data from [21] Congruent with experimental, calculated for  $B_{\text{ext}}=0$   $B_{\text{ext}}=2.0\text{T}$  and  $B_{\text{ext}}=6.0\text{T}$  lines are solid lines.

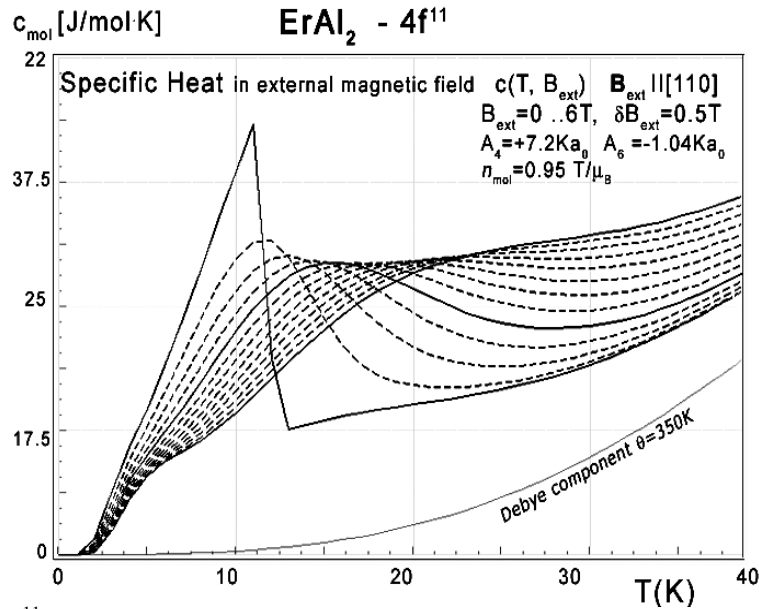


Figure 35. Calculated  $4f^{11}$ -electronic system component of molar specific heat (14) with Debye crystal lattice component ( $\theta=350\text{K}$ ) vs. temperature of Er ions in  $\text{ErAl}_2$ , under the influence of external magnetic field from 0 to 6T with step 0.2T.

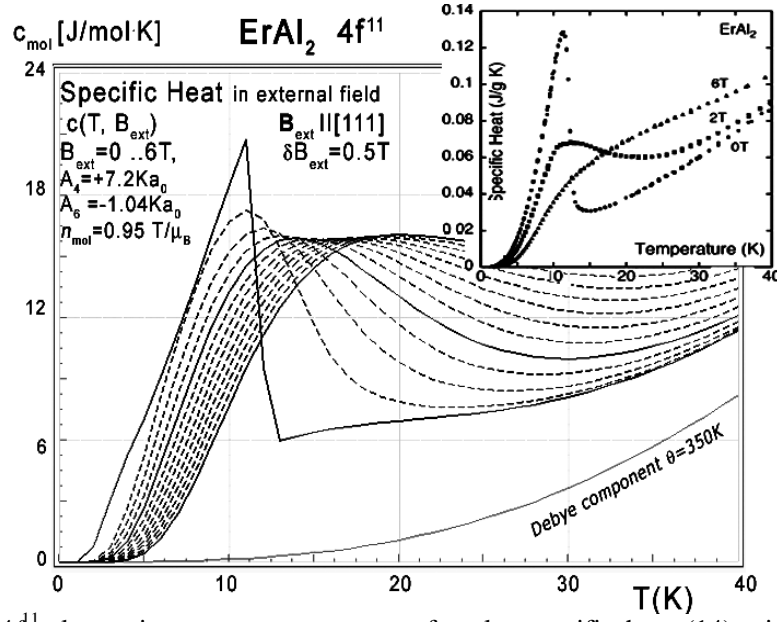


Figure 36. Calculated  $4f^{11}$ -electronic system component of molar specific heat (14) with Debye crystal lattice component ( $\theta=350K$ ) vs. temperature of Er ions in ErAl<sub>2</sub>, under the influence of external magnetic field from 0 to 6T with step 0.2T. Inset: experimental data from [21] Congruent with experimental, calculated for  $B_{ext}=0$   $B_{ext}=2.0T$  and  $B_{ext}=6.0T$  lines are solid lines.

Collected specific heat data makes it possible to calculate isothermal entropy change  $-\Delta S(T, B_{ext})$  according to (16), the same methodology as used by experimentalist [3-8]. Isothermal entropy change calculated with various external magnetic fields is presented in figures 37, 38 and 39.

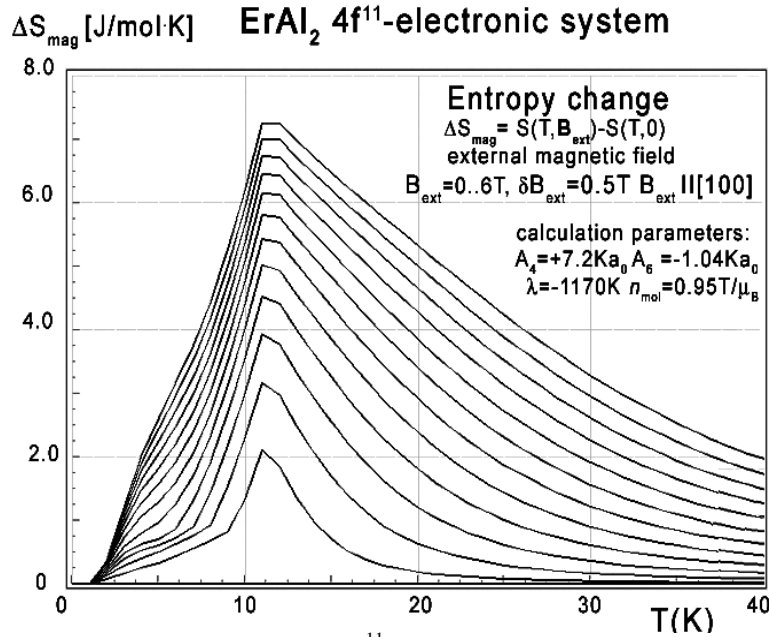


Figure 37. Calculated isothermal entropy change of  $4f^{11}$ -electronic system vs. temperature (16) of Er ions in ErAl<sub>2</sub>, under influence of various values of external magnetic field from 0 to 6T, with step 0.2T applied along [100] direction.

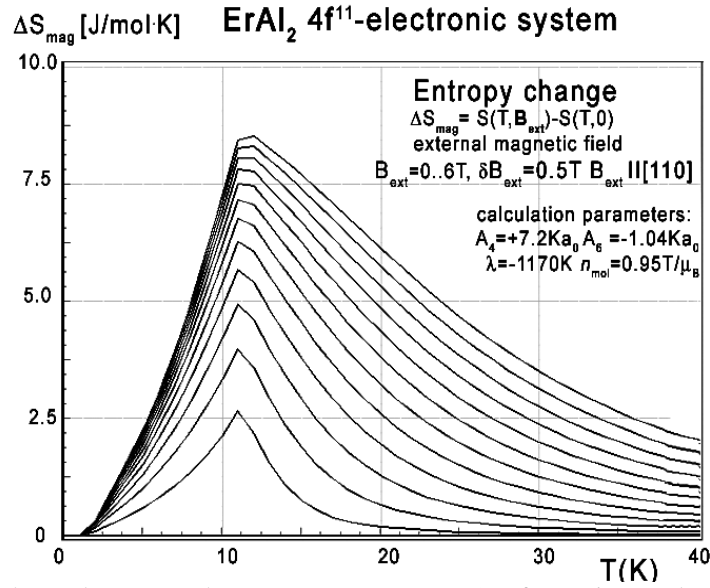


Figure 38. Calculated isothermal entropy change vs. temperature (16) for various values of external magnetic field from 0 to 6.0T with step 0.5T, applied along [110] direction of ErAl<sub>2</sub> crystal lattice.

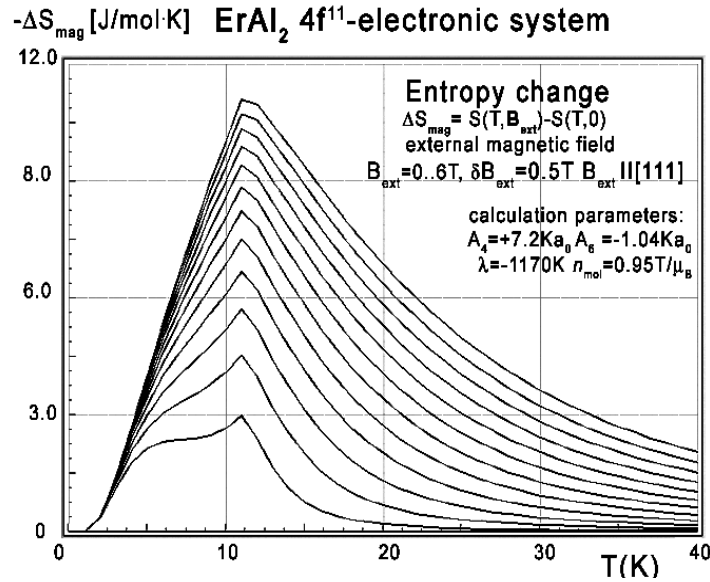


Figure 39. Calculated isothermal entropy change of ErAl<sub>2</sub> vs. temperature (16) for various values of external magnetic field from 0 to 6T with step 0.5T, applied along diagonal [111] direction.

The anisotropic behavior of calculated thermomagnetic properties reflects in magnetocrystalline anisotropy constant calculations. The results of  $K_i(T)$  calculations according to (17) in absence of external magnetic field are shown on figure 40.

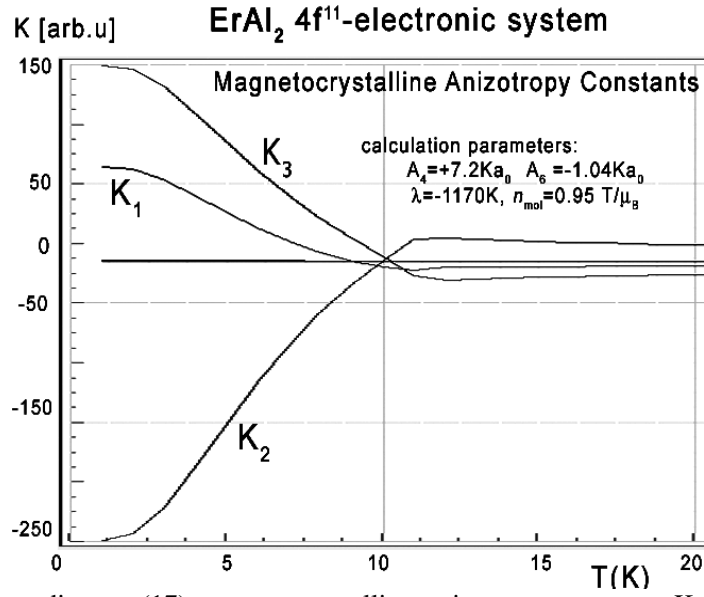


Figure 40. Calculated according to (17) magnetocrystalline anisotropy constants  $K_1, K_2$  and  $K_3$  vs. temperature, calculated for Er ions under influence of CEF established for RAl<sub>2</sub> series and molecular magnetic field.

For completeness, magnetic moment calculations vs. temperature under various external magnetic field conditions was performed. The results of  $\mathbf{m}(T, \mathbf{B}_{ext})$  are presented in figures 41, 42 and 43.

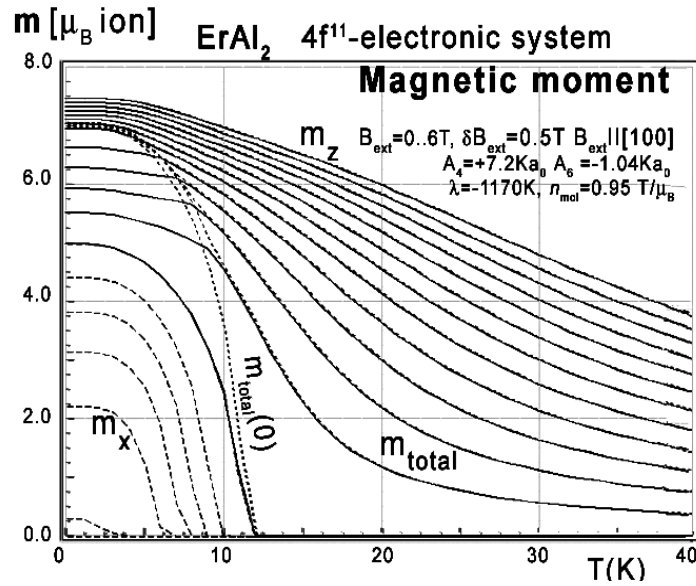


Figure 41. Calculated x,y,z-directional components of total magnetic moment vs. temperature, calculated for Er ions in ErAl<sub>2</sub> under influence of CEF and molecular magnetic field and various values of external magnetic field from 0 to 6T with step 0.5T applied along direction [100].

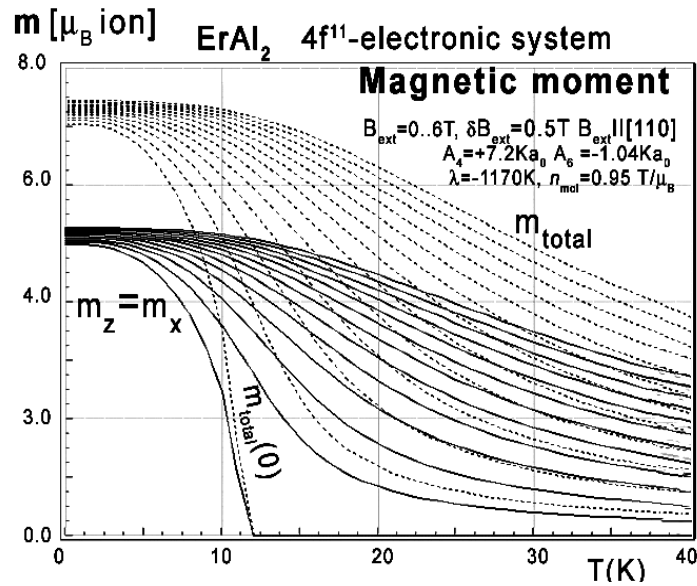


Figure 42. Calculated x,y,z - components of total magnetic moment  $m_{\text{total}}$  (dotted lines) vs. temperature, calculated for Er ions in  $\text{ErAl}_2$  under influence of CEF, molecular magnetic field and various values of external magnetic field from 0 to 6 T with step 0.5 T applied along direction [110].  $m_y(T)=0$ , x and z – components of magnetic moment are equally distributed.

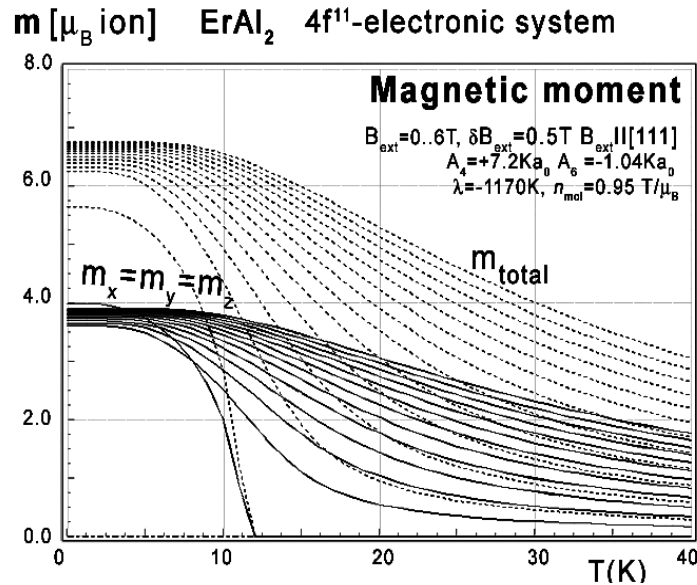


Figure 43. Calculated x,y,z - components of total magnetic moment  $m_{\text{total}}$  (dotted lines) vs. temperature, calculated for Er ions in  $\text{ErAl}_2$  under influence of CEF, molecular magnetic field and various values of external magnetic field from 0 to 6 T with step 0.5 T applied along direction [111]. All directional magnetic moment components are equally distributed.

Magnetic moment calculated in external magnetic field parallel to [111] and [110] direction reveals unusual behavior of the directional component of total moment. The electronic system seems to be easy switchable between those crystallographic directions. The low temperature easy magnetization axis along direction [110] easy transforms into [111]. The external magnetic field under  $B_{\text{ext}} < 0.01 \text{ T}$  changes directional components distribution of total magnetic moment of Er ions (compare figure 42 and figure 43).

Similar behavior of magnetic moment directions was reported in ref. [7], but most of the presented results of calculations of properties of  $\text{ErAl}_2$  still await experimental verification.

## 6. Conclusions

We performed calculations for DyAl<sub>2</sub> thermomagnetic properties with the ATOMIC MATTERS MFA computation system. The local symmetry of the Dy ions is cubic, which significantly simplifies the analyses. All the calculations were performed with 2 only cubic CEF parameters and molecular field factor  $n_{mol}$ . The excellent agreement obtained between the calculated thermomagnetic properties and the reference data confirms the effectiveness of our theoretical approach.

According to established universal CEF parameters ( $A_n^m$ ) for all RaAl<sub>2</sub> compounds we performed similar calculations for HoAl<sub>2</sub> and ErAl<sub>2</sub> thermomagnetic properties. The local symmetry of the Ho and Er ions is cubic, which significantly simplifies the analyses. All the calculations were performed without free parameters. Very good agreement was obtained between thermomagnetic properties and experimental data. This confirms the effectiveness of our theoretical approach. Working with ATOMIC MATTERS MFA revealed its high usefulness. The visual form of calculation results, full 3D interactive CEF potential visualization, intuitive tools for convention and unit recalculation, and the ability to compare data results all allow the user to utilize the power of the application very effectively. In conclusion, we confirm that ATOMIC MATTERS MFA is a unique application that combines a package of tools for correctly describing the physical properties of atomic-like electron systems subjected to electromagnetic interactions in real materials. This is an accurate tool for calculating properties of ions under the influence of the electrostatic potential of definable symmetry and both external and inter-ionic magnetic fields taken as a mean field approximation in magnetically ordered state. This paper is the first in a series devoted to the RAl<sub>2</sub> (R=rare earth) compounds family non-free parameters calculations.

#### References:

- [1] Michalski R and Zygałło J 2016 Describing the Fine Electronic Structure and Predicting Properties of Materials with ATOMIC MATTERS Computation System *Proceedings: 18<sup>th</sup> Int. Conf. on Physics, Mathematics and Computer Science - Dubai UE* <http://waset.org/publications/10004653/pdf>
- [2] Michalski R and Zygałło J 2016 Thermal dependences of single ionic, magnetic properties of materials in ordered state, calculated with ATOMIC MATTERS MFA computation system *Proceedings: 7<sup>th</sup> IIF-IIR International Conference on Magnetic Refrigeration at Room Temperature, Thermag VII - Torino ITALY*
- [3] Lima A L, Tsokol A O, Gschneidner K A Jr, Pecharsky V K, Lograsso T A and Schlagel D L 2005 *Phys. Rev. B* **72** 024403
- [4] Purwins H G and Leson A 1990 *Adv. Phys.* **39** 309
- [5] Pecharsky V K, Gschneidner K A, Pecharsky A O and Tishin A M (2001) *Phys. Rev. B* **64** 144406
- [6] von Ranke P J, de Oliveira N A, Plaza E J R, de Sousa V S R, Alho B P, Magnus A, Carvalho G, Gama S and Reis M S 2008 *Journal Of Applied Physics* **104** 093906
- [7] Gil L A, Campoy J C P, Plaza E J R and de Souza M V 2016 *Journal of Magnetism and Magnetic Materials* **409** 45–49
- [8] Patra M, S. Majumdar S, Giri S, Xiao Y and Chatterji T 2011 Magnetic and magnetoresistive properties of cubic Laves phase HoAl<sub>2</sub> single crystal *arXiv:1107.1975* [cond-mat.mtrl-sci]
- [9] Blaut A, Michalski R, Kocor M, Ropka Z, Baran A J and Radwanski R J 2003 *Acta Physica Polonica B* **34** 1261-1264
- [10] Software website: [www.atomicmatters.eu](http://www.atomicmatters.eu)
- [11] Rudowicz C and Chung C Y 2004 The generalization of the extended Stevens operators *J. Phys.: Condens. Matter* **16** 5825–5847
- [12] Hutchings M T 1964 *Solid State Phys.* **16** New York
- [13] Franse J J M and Radwanski R J 1993 Magnetic properties of binary rare-earth... in *Handbook of Magnetic Materials* Vol 7, ed Bushow K H J 307-500
- [14] Radwański R J, Michalski R, Ropka Z and Blaut A 2002 *Physica B* **319** 78–89
- [15] Szpunart B and Lindgard P A 1979 *J. Phys. F: Metal Phys.* Vol. **9** No. 3
- [16] de Gennes P G 1962 *J.Phys.Radiat* **23** 5010
- [17] Wybourne B G 1970 *Symmetry Principles and Atomic Spectroscopy* J. Wiley and Sons New York
- [18] Abragam A and Bleaney B 1970 *EPR of Transition Ions*, Clarendon Press, Oxford
- [19] Wang F W, Zhang X X and Hu F X 2000 *Appl. Phys. Lett.* Vol. **77** No. 9 1360
- [20] Ribeiro P O, Alho B P, Alvarenga T S T, Nóbrega E P, deSousa V S R, Magnus A, Carvalho G, Caldas A, deOliveira N A and von Ranke P J 2015 *Journal of Magn. Magn. Mater.* **379** 112–116
- [21] Wikusa P, Canavan E, Heine S T, Matsumoto K and Numazawa T 2014 *Cryogenics Preprint*



## Predictions of thermomagnetic properties of Laves Phase compounds: TbAl<sub>2</sub>, GdAl<sub>2</sub> and SmAl<sub>2</sub> performed with ATOMIC MATTERS MFA Computation System

Rafał Michalski <sup>a,\*</sup>, Jakub Zygałło <sup>b</sup>

<sup>a</sup> Atomic Systems, M. Pszona 41/29, Cracow, Poland

<sup>b</sup> Faculty of Mathematics and Computer Science, Jagiellonian University, Cracow, Poland

### *Highlights:*

- Calculated Fine Electronic Structure of TbAl<sub>2</sub> reveals its unusual thermomagnetic properties, sensitive for direction and value of external magnetic field.
- Fine Electronic Structure of 4f<sup>5</sup> electronic configuration of Sm<sup>3+</sup> ions reveals Spin and Orbital moment compensation in cubic structure of SmAl<sub>2</sub>.
- Evidence of fundamental role of Crystal Electric Field (CEF) and spin-orbit coupling for thermomagnetic properties of RAl<sub>2</sub> (R=Rare Earth) Compounds.
- Mean Field Approximation (MFA) approach for description of single ionic, magnetic properties of materials around phase transition temperature is fully agreed with experimental data for TbAl<sub>2</sub> and GdAl<sub>2</sub>.

**Keywords:** TbAl<sub>2</sub>, GdAl<sub>2</sub>, SmAl<sub>2</sub>, Crystal Field, Atomic Matters, CF, CEF, MFA

---

\* Corresponding author at: Atomic Systems, Cracow, Poland

E-mail address: r.michalski@induforce.eu